Bioconjugate Chemistry

Review

pubs.acs.org/bc

Biomarkers and Molecular Probes for Cell Death Imaging and Targeted Therapeutics

Bryan A. Smith and Bradley D. Smith*

Department of Chemistry and Biochemistry, Notre Dame Integrated Imaging Facility, 236 Nieuwland Science Hall, University of Notre Dame, Notre Dame, Indiana 46556, United States

ABSTRACT: Cell death is a critically important biological process. Disruption of homeostasis, either by excessive or deficient cell death, is a hallmark of many pathological conditions. Recent research advances have greatly increased our molecular understanding of cell death and its role in a range of diseases and therapeutic treatments. Central to these ongoing research and clinical efforts is the need for imaging technologies that can locate and identify cell death in a wide array of in vitro and in vivo biomedical samples with varied spatiotemporal requirements. This review article summarizes community efforts over the past five years to identify useful biomarkers for dead and dying cells, and to develop molecular probes that target these biomarkers for optical, radionuclear, or magnetic resonance imaging. Apoptosis biomarkers are classified as either intracellular (caspase enzymes, mitochondrial membrane potential, cytosolic proteins) or extracellular (plasma membrane phospholipids, membrane potential, surface exposed histones). Necrosis, autophagy, and senescence biomarkers are described, as well as unexplored cell death biomarkers. The article discusses possible chemotherapeutic and theranostic strategies, and concludes with a summary of current challenges and expected eventual rewards of clinical cell death imaging.

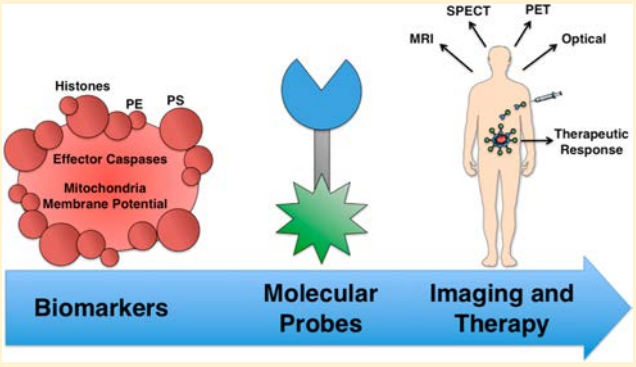

INTRODUCTION

Cell death is an essential biological process that plays a vital physiological and pathological role within an organism. Programmed cell death is critical for the correct formation of organs and tissues during development and also functions to rid the body of cells that have been infected or damaged by pathogens. During our lifetime, over 99.9% of our cells will undergo cell death and be eliminated by the body, thus providing an important mechanism for maintaining homeostasis and a process for fighting disease.[1] Disruption of homeostasis, either by excessive or deficient cell death, is a hallmark of many pathological conditions including cancer, neurodegenerative disorders, cardiovascular diseases, autoimmune diseases, and others that are listed in Figure 1.[2,3]

Cell death is often divided into two distinctive processes, apoptosis and necrosis; however, there is increasing evidence for additional pathways such as autophagy, mitotic catastrophe, and senescence.[4−8] Apoptosis is characterized by classical morphology changes such as cytoplasm shrinkage, cell detachment, chromatin condensation, nuclear fragmentation, and the formation of apoptotic bodies. In contrast, necrotic cells exhibit increased cytoplasmic vacuolation, organelle degeneration, condensation of chromatin into irregular patches, and an increase in cell volume that results in irreversible rupture of the plasma membrane. Biochemically, apoptotic cell death includes activation of caspases, mitochondrial outer membrane permeabilization, DNA fragmentation, generation of reactive oxygen species (ROS), lysosomal membrane permeabilization (LMP), and exposure of molecular biomarkers such as phosphatidylserine (PS) on the outer leaflet of the plasma membrane. Unambiguous assignment of a cell death process is a challenging task, since different death processes can induce

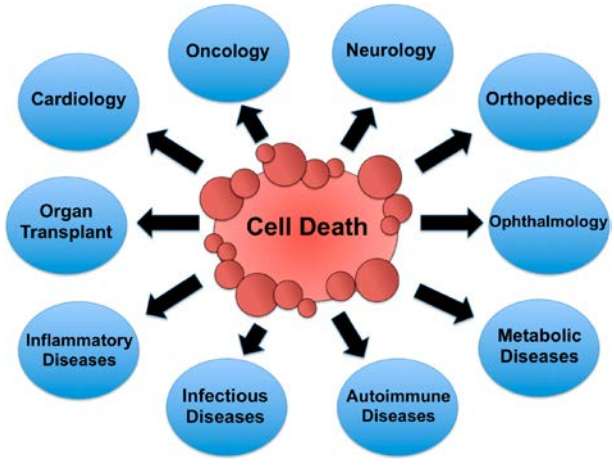

Figure 1. Medical fields and diseases that are associated with dysregulation of cell death.

Received: June 20, 2012
Revised: September 2, 2012
Published: September 18, 2012

the same change in one biomarker. For example, PS exposure, ROS generation, and LMP are biomarkers associated with both apoptosis and necrosis.[9−11] There is also evidence for crosstalk between multiple death processes that are occurring simultaneously.[12]

The ongoing efforts of a large international group of biomedical researchers are greatly expanding the collective understanding of cell death and its role in a range of diseases and therapeutic treatments. Central to these research and clinical efforts is the need for imaging and detection technologies that can locate and identify cell death in a wide array of in vitro and in vivo biomedical samples with vastly different spatiotemporal requirements (Figure 2). Ideally, these

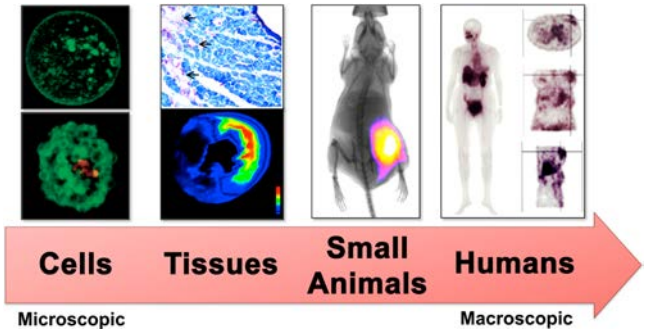

Figure 2. Cell death imaging is conducted on various biomedical subjects ranging from cells to humans. Reprinted with permission from refs 3,76,89,117.

technologies should be able to quantify the biomarkers that are specific for each cell death process. A common strategy for effective molecular imaging, especially in the clinic, is to employ a suitably designed molecular probe that is composed of a targeting group conjugated to a reporter group. In addition to the normal probe development challenges of obtaining high target selectivity and sensitivity, cell death imaging has the additional complication that it is a time-dependent process (Figure 3). A high-contrast image must be achieved within a specific window in time that will depend on the specifics of the cell death phenomenon under study. Therefore, a single cell death imaging probe will not likely be applicable for all types of imaging problems. A more realistic solution is a palette of cell death imaging methods with complementary operational attributes. The goal of this review is to summarize recent

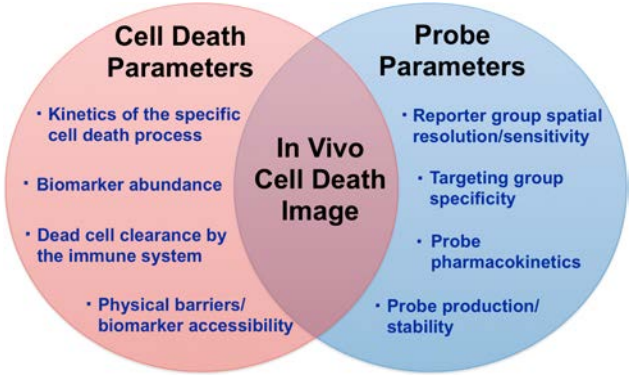

Figure 3. Development of a successful in vivo imaging probe for cell death requires global optimization of a large set of interdependent parameters.

community efforts to identify useful cell death biomarkers for each type of cell death process and to develop molecular imaging probes and therapeutics that target these biomarkers. The focus is on methods that allow imaging of cell culture or living animals, and the scope does not include diagnostic assays or stains for biopsy or histopathology sections. Also not discussed are imaging methods that monitor changes in uptake of molecular probes for cell metabolism (e.g., ^{18}F-FDG, ^{11}C-choline) or cell proliferation (e.g., ^{18}F-FLT).[13,14] The emphasis is on recent advances that have occurred within the last five years; thus, the article builds on previous reviews.[15−20]

CURRENT CELL DEATH BIOMARKERS AND IMAGING MODALITIES

In Figure 4 is a short summary of currently validated cell death biomarkers for molecular imaging. A more detailed listing in

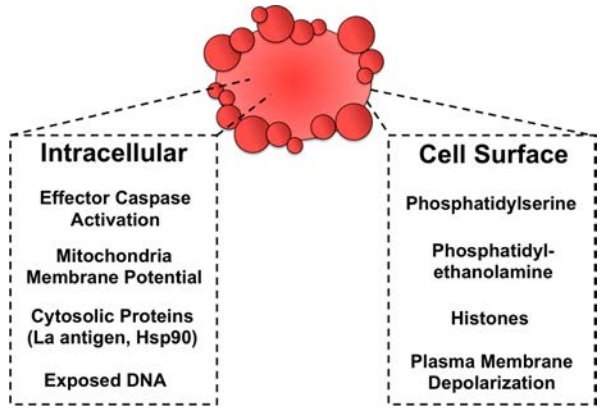

Figure 4. Validated intracellular and extracellular biomarkers for cell death imaging.

Table 1 contains additional information including the imaging modality. Most cell death imaging studies employ one of three modalities: optical, radionuclear, or magnetic resonance imaging. These modalities have complementary properties that make them suitable for different types of in vivo imaging applications (Table 2).[21] Optical imaging can be broken into two groups, fluorescence and bioluminescence. Fluorescence is well-suited for diagnostic and microscopy studies of cells and tissue sections. A rich assortment of targeted fluorescent probes has been developed, including fluorescent reagents that are activated by enzymes.[22]

Bioluminescence imaging utilizes cells that have been genetically engineered to convert chemical fuel into light. This modality does not require an external light excitation source; thus, sensitivity and signal-to-noise ratios are typically greater than fluorescence imaging.[23] For in vivo studies of living animals, a major weakness with optical methods is the poor penetration of visible light through skin and tissue. This technical problem is mitigated by employing imaging probes or cells that emit deep-red or near-infrared light, but the light is scattered as it passes through the sample and the resolution of whole-body, live animal optical images is typically quite poor.[24] In comparison, radionuclear imaging methods such as positron emission tomography (PET) and single photon emission computed tomography (SPECT) provide much deeper tissue penetration and greatly reduced scattering of the emitted signal and, thus, are more attractive for many types of clinical applications.[25] However, the high cost, low throughput, and

Table 1. Cell Death Biomarkers and Probe Targeting Groups

biomarker	type of cell death	targeting group	imaging modalities	ref
effector caspases	apoptosis	DEVD sequence[a]	BLI, Fluorescence	30−48
		Isatins[b]	PET	50,51,53,54
		Acyloxymethyl ketones[b]	Fluorescence	56
phosphatidylserine	apoptosis, necrosis	Annexin V[c,e]	Fluorescence, PET, SPECT, MRI, Ultrasound	74−78,80,81,83,85−90,92−94,96,97
		C2A domain of Synaptotagmin[c]	Fluorescence, PET, SPECT,	98−102
		Lactadherin[c]	Fluorescence, SPECT	103−105
		LIKKPF[a]	MRI	106−110
		TLVSSL[a]	MRI	108,109
		CLSYYPSY[a]	Fluorescence	111
		SVSVGMKPSPRP[a]	Fluorescence	112
		FNFRLKAGAKIRFG[a]	Fluorescence, SPECT	113
		cLac-2[a]	Fluorescence	114
		ZnDPA[b]	Fluorescence, SPECT, MRI	115−124
		Zn-cyclen[b]	Fluorescence, PET	125
phosphatidylethanolamine	apoptosis, necrosis	Duramycin[a]	Fluorescence, SPECT	127−129
histones	apoptosis	CQRPPR (Apopep-1)[a]	Fluorescence, PET	137,138,207,208
mitochondrial membrane potential	apoptosis	Phosphonium cations[b]	PET	64,65
la antigen	late apoptosis, necrosis	La mAb 3B9[d]	Fluorescence, SPECT	68,69
		APOMAB DAB4[d]	SPECT	70
heat shock proteins	late apoptosis, necrosis	GSAO[b]	SPECT	71
autophagosome	autophagy	LC3[c]	Fluorescence	174−177
exposed DNA	necrosis	Hoechst-IR[b]	Fluorescence	150
		Gd-TO[b]	Fluorescence, MRI	151,152
plasma membrane depolarization	apoptosis	DDC[b]	Fluorescence	139−141
		ML-10[b,e]	Fluorescence, PET	144−147
		DFNSH[b]	Fluorescence, PET	142,143
unknown	necrosis	Hypericin[b]	Fluorescence, PET, SPECT,	154−156,158,159
		Pamoic Acid[b]	PET, SPECT	160,161
		bis-DTPA-BI[b]	SPECT	162

[a]Peptide. [b]Small molecule. [c]Protein. [d]Antibody. [e]Clinical studies.

safety concerns associated with radionuclear imaging can be serious drawbacks. Magnetic resonance imaging (MRI) does not employ ionizing radiation and can produce high-resolution images of deep-tissue sites, but the technique is relatively insensitive.[26] Overall, optical imaging is often used for preclinical research studies employing cells or small animal models, whereas radionuclear and MRI are more suitable for most types of clinical imaging.

APOPTOSIS BIOMARKERS

Intracellular Apoptosis Biomarkers. *Caspases.* Caspases are a family of intracellular cysteine proteases that play an important role in the initiation and execution of apoptosis.[27] Caspases are typically divided into initiators (caspase-8, -9, and -10) that start the apoptotic cascade and effectors (caspase-3, -6, and -7, also known as executioner caspases), which are activated by the initiators. Furthermore, initiators are divided into caspases that participate in either the extrinsic (caspase-8 and -10) or intrinsic (caspase-9) apoptotic pathway.[28] Within the cell, caspases exist as zymogens that are converted by a pro-apoptotic signal into an active form. Initiator caspases are activated by homodimerization, whereas effector caspases are activated by cleavage of a catalytic domain.

Caspases selectively cleave protein or peptide amide bonds that are on the carboxyl side of aspartic acid residues. The catalytic mechanisms are similar to other cysteine proteases, and studies are ongoing to fully understand the molecular processes producing the enzyme activation, bond cleavage, and enzyme inhibition.[29] There are no clear-cut rules that predict the optimal substrate sequence selectivity for a specific caspase, but typically, initiator caspases recognize and cleave WEHD sequences while effector caspases recognize the DEVD motif.[28] The specificity of effector caspases for the DEVD sequence has been exploited by researchers to produce activatable molecular probes for optical imaging of apoptosis. The simplest molecular design incorporates a fluorescent donor/acceptor energy transfer pair that is separated by a cleavable peptide sequence.[30] Cleavage of the peptide disconnects the energy transfer and switches on the fluorescence emission signal only at spatial locations with high caspase levels. This imaging strategy has proven quite useful for high-throughput screening of drug candidates in cell systems[31] and microscopic visualization of chemotherapy-induced apoptosis in disseminated tumors.[32] Deployment of the method for in vivo imaging of apoptosis requires caspase activatable probes with two additional attributes, (a) ability to emit near-infrared light, and (b) ability to penetrate the cell cytosol within the time frame for caspase activation.[33] Both requirements were addressed in a study by Bullock et al. who synthesized a cell permeable activatable caspase substrate consisting of an all D-amino acid cell permeation peptide, RKKRRORRRG, conjugated to the N-terminus DEVDAPC caspase sequence. The recognition

dx.doi.org/10.1021/bc3003309 | Bioconjugate Chem. 2012, 23, 1989−2006

Table 2. Strengths and Weaknesses of In Vivo Imaging Modalities

imaging modality	strengths	weaknesses
Fluorescence	High sensitivity	Low resolution
	Low cost	Low depth penetration
	High-throughput	Limited clinical translation
	Easy to perform	
	Large number of available probes	
	Able to monitor two or more probes simultaneously	
Bioluminescence	High sensitivity	Low resolution
	Low background signal	Need for genetic modification
	High-throughput	Limited clinical translation
	Easy to perform	
	Multispectral imaging	
PET	High sensitivity	Cost
	Unlimited depth penetration	Limited spatial resolution
	Clinical translation	Unable to monitor two or more probes simultaneously
SPECT	Unlimited depth penetration	Cost
	Clinical translation	Limited spatial resolution
	Able to monitor two or more probes simultaneously	Limited sensitivity
MRI	High spatial resolution	Cost
	Clinical translation	Low sensitivity
		Imaging time

sequence was then flanked by a deep-red fluorophore and a spectral quencher to produce TcapQ$_{647}$. The probe fluorescence was specifically activated by effector caspases and not initiator caspases, and was effective in cell culture and also amoeba-induced tumor cell death.[34] This probe was also used to image single-retinal ganglion cell apoptosis in an in vivo rat model of glaucoma.[35] The same research group produced a second-generation cell-penetrating caspase-activatable probe that contained a lysine-arginine-rich (KKKRKV) cell-penetrating peptide sequence and an L-amino acid cleavable domain.[36] This probe had essentially the same specificity and diagnostic properties as the first generation, TcapQ, but it was more biocompatible.

Polymer and nanoparticles are promising alternative scaffolds for enzyme activated imaging probes because they can present multiple fluorescent reporter groups and thus produce large changes in optical signal. The fluorophores are strongly self-quenched when they are attached to the scaffold, and a strong signal enhancement is produced when they are released by caspase cleavage. Strategies utilizing gold nanoparticle systems[37−39] and self-assembly nanostructures[40] have enabled direct observation of effector caspase activation and apoptosis in living cells. While all of these systems focus on measuring effector caspase activity, Huang and co-workers developed a nanoquencher system that could monitor the activities of different caspases simultaneously.[41] The nanoquencher was generated by incorporating different dark quenchers into a mesoporous silica nanoparticle, and then conjugating the nanoparticle with a set of fluorescent peptide substrates that were responsive to different caspases. Thus, the fluorescence is turned on at wavelengths that are specific to the caspase that is activated. Using multiplexed fluorescence microscopy, the nanoquencher enabled simultaneous visualization of caspase-8, caspase-9, and caspase-3 activation after TRAIL-induced apoptosis in HCT116 cells. Moreover, the system returned to a relatively "dark" state upon addition of caspase-8, caspase-9, and caspase-3 inhibitors, highlighting the high enzyme specificity.

Bioluminescence imaging can be achieved using the luciferase enzyme to promote an oxidation reaction, which in turn produces light that can be captured by a sensitive camera. The most common strategy for designing bioluminescent apoptosis constructs is to restore luciferase activity through structural changes upon caspase activation[42] (a less common, alternative approach is to utilize BRET, bioluminescence resonance energy transfer[43]). Kanno et al. achieved luciferase activity restoration by designing a genetically encoded cyclic construct containing two fragments of a DnaE intein fused to the neighboring ends of FLuc connected by a DEVD sequence. Once translated, the cyclic peptide distorts the structure of the luciferase causing it to lose bioluminescence activity.[44] Cleavage by a caspase-3 enzyme converts the luciferase back to its active form and restores its activity. The cyclic luciferase was able to provide quantitative measurements of caspase-3 activity in response to external stimuli both in vitro and in a living rodent. Ray et al. developed a fusion protein, which encoded three different reporter proteins (producing bioluminescent, red fluorescent, and PET signals) linked by a DEVD peptide that can be specifically cleaved by active caspase-3. When tumor xenografts expressing this vector were treated with staurosporine, both the luciferase activity and the thymidine kinase PET activity increased by 2-fold compared to controls.[45] In a similar fashion, Niers et al. developed an apoptosis biosensor by using a caspase-3 cleavable sequence to link a green fluorescent protein to a *Gaussia* luciferase. The reporter was capable of monitoring apoptosis in real-time assays of whole blood.[46] A different approach was taken by Coppola et al. who adapted a split-firefly reporter to construct a fusion of N- and C-termini of luciferase connected by a caspase-3 cleavage site.[47] During apoptosis, caspase-3 cleaves the dark construct, which allows the two peptides to interact and restore luciferase activity through protein complementation. Treatment studies with tumor-bearing mice showed the utility of this reporter to report on the efficacy of combination and experimental therapies through dynamic, noninvasive imaging. In an alternate strategy, Promega Inc. developed a modified FLuc luciferase substrate, Z-DEVD-aminoluciferin, that acts as a luciferase substrate only when caspase-3 is activated and cleaves the DEVD sequence. Hickson et al. employed this technology to detect caspase-3 activation in response to chemotherapy in two preclinical oncology models without toxicity to the animals.[48] While bioluminescence imaging of caspase responsive reporters has attractive features for preclinical research, a central limitation for clinical translation is the need to genetically modify the cells of interest and introduce them into a living animal.

A promising approach to nuclear imaging of caspase activity employs selective and high affinity caspase inhibitors. Isatins are small molecule covalent inhibitors of activated caspase-3 and caspase-7 and thus attractive probe molecules for apoptosis imaging.[49] Nguyen et al. synthesized a radiolabeled isatin 5-sulfonamide ([^{18}F]ICMT-11) that was previously identified to have subnanomolar affinity for caspase-3.[50,51] The study showed that increased cellular uptake of [^{18}F]ICMT-11 in vitro and in drug-treated tumors was associated with an

dx.doi.org/10.1021/bc3003309 | *Bioconjugate Chem.* 2012, 23, 1989−2006

increase in caspase-3/7 activity. The study also suggested that [^{18}F]ICMT-11 PET imaging may be useful for monitoring response to therapy in nonabdominal malignancies since there was high retention in the liver and intestines. [^{18}F]ICMT-11 has recently been selected by the QuIC-ConCePT consortium for evaluation in humans as a candidate cell death imaging probe.[52] Other researchers have reported new synthetic procedures to produce radiolabeled isatin analogues and identified promising probe structures that accumulate in mouse models of liver cell death.[53,54] Another class of caspase inhibitors are peptide acyloxymethyl ketones, which work by alkylating the enzyme active site cysteine residue.[55] Edgington et al. developed fluorescently labeled acyloxymethyl ketone probes that bound irreversibly to the active site of caspase-3/7 and allowed noninvasive in vivo imaging of apoptosis kinetics in multiple mouse models.[56]

While caspases are well-known as apoptosis biomarkers, it is important to realize that the biological functions of caspases can extend beyond apoptosis and include other cellular remodeling events. Caspase activation is required for erythropoiesis and the differentiation of keratinocytes, lens epithelial cells, and neurons.[57,58] Moreover, caspase-3 can regulate B-cell proliferation and recently has been implicated in stem cell maintenance and differentiation.[59] The DEVD peptide sequence can also be cleaved by other cysteine proteases such as cathepsins and legumain.[60] As a precaution, researchers should complement caspase imaging with other biochemical techniques to ensure that they are monitoring caspase activity related to apoptosis.

Mitochondrial Membrane Potential. Mitochondria play a key role in the apoptotic cascade and a loss of membrane potential across the inner mitochondrial membrane ($\Delta\psi_m$) accompanies the induction of cell death.[61] Lipophilic phosphonium cations are known to penetrate healthy cells and accumulate at mitochondrial membranes that have a strongly negative transmembrane potential.[62] During apoptosis, the electrochemical proton gradient across the inner mitochondrial membrane collapses causing a reduction in phosphonium cation tracer levels.[63] The ^{18}F-fluorobenzyl triphenylphosphonium cation (^{18}F-FBnTP) has been investigated as a PET imaging probe to detect alterations in mitochondrial membrane potential in vitro and in vivo. ^{18}F-FBnTP was used to measure the pharmacodynamics of paclitaxel treatment in breast cancer cells, and the decrease in ^{18}F-FBnTP uptake coincided with other apoptotic biomarkers such as Bax expression and cytochrome c release.[64] A preclinical orthotopic prostate tumor treatment study showed significantly lower uptake of ^{18}F-FBnTP into a treated tumor compared to ^{18}F-FDG, a standard glucose-based probe that is used to measure the metabolic index of tumors.[64] These studies required excision of tissues and ex vivo audioradioagraphy in order to obtain ^{18}F-FBnTP quantification. Future studies will need to employ noninvasive, whole-body PET imaging to determine if ^{18}F-FBnTP can accurately measure the kinetics and extent of apoptosis in a living animal. Biodistribution studies in healthy animals showed high ^{18}F-FBnTP uptake in the kidneys, heart, and liver suggesting that these organs would provide a high starting signal for detection of apoptotic-related decreases.[65] Nonetheless, imaging methods that are based on signal decreases are technically less attractive than methods that are based on signal increases.

Other Intracellular Apoptosis Biomarkers. Although effector caspases are the most studied intracellular cell death biomarker, there is ongoing effort to identify other intracellular proteins as targets for cell death imaging.[66] The La antigen is an abundant protein that acts as a molecular chaperone for RNA polymerase III. La is believed to play an important role in the coupling of transcription and translation by acting as a shuttle between the nucleus and cytoplasm.[67] La is overexpressed in human malignant cells compared to normal cells, and an La-specific monoclonal antibody (3B9) is able to identify this difference in expression levels.[68] In vitro and in vivo studies showed that the accumulation of 3B9 in the cytoplasm of dead cancer cells correlates with increasing DNA damage.[69] For this method to work successfully, the following biochemical steps have to occur: (1) overexpression of La in malignant cells, (2) cleavage and redistribution of the La antigen to the cytoplasm after DNA-damaging treatment, (3) antibody permeation through the disrupted membranes of dead/dying cells, and (4) "fixation" of the La antigen and 3B9 by transglutaminase 2-mediated protein cross-linking, which occurs during cell death.[68] Subsequent studies of a radiolabeled La-specific monoclonal antibody, APOMAB DAB4 clone, showed an ability to detect chemotherapy induced tumor apoptosis.[70] In a conceptually related manner, the 90 kDa heat shock protein (Hsp90) has also been targeted by a radiolabeled trivalent arsenical peptide, 4-(*N*-(*S*-glutathionylacetyl)amino)-phenylarsonous acid (GSAO) for noninvasive identification of tumor cell death.[71] Hsp90 contains a pair of highly conserved cysteines (Cys719 and Cys720) that can be selectively cross-linked by the GSAO probe. The high abundance of Hsp90 makes it an attractive target for sensitive molecular imaging; however, it appears that the cell membrane must be partially compromised for GSAO entry. It is not precisely known when, and by how much, plasma membrane permeability changes as a cell progresses from early- to late-stage apoptosis. The plasma membrane of an apoptotic cell has high integrity and is permeable to only a select group of small molecules, including nucleotides and cyanine dyes (due in part to caspase-mediated activation of the membrane channel protein, pannexin 1).[72] In contrast, the plasma membrane of a necrotic cell is completely disrupted with free access of small and large molecules to the cell interior.

Extracellular Apoptosis Biomarkers. *Plasma Membrane Phospholipids.* The plasma membrane of healthy mammalian cells has an asymmetric distribution of phospholipids. The membrane outer leaflet is composed primarily of the zwitterionic phospholipids, phosphatidylcholine, and sphingomyelin, and the exterior membrane surface is close to charge-neutral. Sequestered within the plasma membrane inner leaflet are phosphatidylethanolamine (PE) (20−40% of total phospholipid) and the major anionic phospholipid, phosphatidylserine (PS) (2−10% of total phospholipid). Loss of this asymmetric distribution during cell death, cell activation, or cell transformation leads to PS and PE exposure and the cell surface becoming anionic. The appearance of PS and PE on the cell surface appears to be a universal indicator of most types of cell death processes and thus high abundance biomarkers for cell death imaging.[73]

There has been extensive effort to develop targeted imaging probes for exposed PS using appropriately labeled PS-binding proteins.[19] The most studied PS-binding protein is annexin V, a 36 kDa single chain protein that binds to PS in a Ca^{2+}-dependent manner. Annexin V derivatives have been developed for in vivo imaging using SPECT,[74] PET,[75] MRI,[76] ultrasound,[77] and fluorescence[78] modalities and several have reached clinical trials.[79] Although many studies have produced

dx.doi.org/10.1021/bc3003309 | *Bioconjugate Chem.* 2012, 23, 1989−2006

promising results, there appear to be lingering technical questions about nonideal pharmacokinetics and probe production.[80−83] It is known that covalent attachment of different labels (e.g., fluorescent dyes, chelators for radionuclides) can significantly change the protein's binding properties and pharmacokinetics. The most studied conjugate of annexin V is ^{99m}Tc-hydrazinonicotinamide-annexin V (^{99m}Tc-HYNIC-annexin V), which has been tested for preclinical and clinical SPECT imaging of tumor response to treatment and other models of cell death.[84,85] The simplest way to attach the HYNIC group is to treat annexin V with N-succinimidyl HYNIC. This method has a drawback in that the native annexin V has 21 lysine residues available for conjugation; thus, there is a statistical distribution of labels. To circumvent this problem, site-directed mutagenesis has been used to produce mutant proteins that can be cleanly labeled with controlled stoichiometry. One approach incorporates a reactive cysteine residue for labeling by thiol conjugation chemistry.[86] Introduction of the cysteine residue did not alter the apoptotic cell binding properties, and the mutant annexin probe showed a high level of kidney retention with lower accumulation in the spleen and liver.[87] Histidine-tagged annexin V variants have also been developed, and both pharmacokinetics and in vivo detection of cell death appear to be very similar to that of ^{99m}Tc-HYNIC-annexin V.[88] Another bioconjugation method attached ethylenedicysteine to annexin V which enabled ^{99m}Tc chelation. Clinical imaging of ten patients with breast cancer showed higher target to nontarget ratios in drug-treated tumors compared to non-treated tumors (Figure 5).[89] The conjugation methods for developing SPECT versions of annexin V have nearly been exhausted; thus, future research to improve pharmacokinetics and clinical utility will likely evolve toward PET versions of annexin V or new targeting strategies.[79] Indeed, specific conjugation methods have been developed to produce ^{68}Ga, ^{11}C, and ^{18}F labeled versions of annexin V for PET imaging.[90−92] Annexin V conjugated with ^{18}F enabled visualization and monitoring of tumor cell death dynamics due to doxorubicin treatment.[93] Furthermore, ^{18}F-annexin V showed high uptake in the spleen and bone marrow of doxorubicin-treated mice, which reflected drug-induced toxicity to these cells.

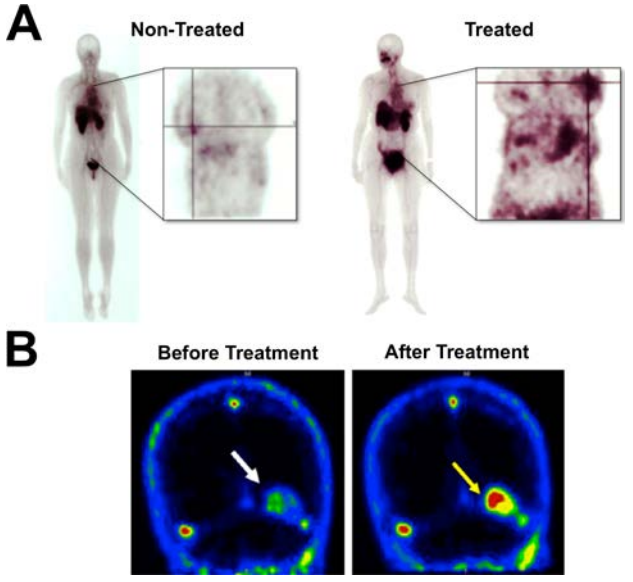

Figure 5. Clinical imaging with cell death molecular probes. (A) Scintigraphic images of separate nontreated and drug treated breast cancer patients who were injected with ^{99m}Tc-EC-Annexin V. Annexin V had higher accumulation in treated breast tumors compared to nontreated tumors, though the probe localized to both tumors as indicated by the cross-lines. (B) ^{18}F-ML-10 PET images of a brain metastasis in a single patient (indicated by arrow) before and after whole brain radiation therapy. The low level of ^{18}F-ML-10 accumulation in the metastasis prior to treatment likely represents a basal amount of cell death. Reprinted with permission from refs 89 and 147.

Recent work to improve annexin V image contrast includes the development of a pretargeting strategy using biotinylated annexin V and radiolabeled streptavidin.[94] The stepwise dosing process starts with an intravenous injection of biotinylated annexin V, which targets dead and dying cells. A subsequent injection of a limited amount of avidin protein rapidly associates with any free annexin V in the blood pool and clears it from the circulation. A third injection of radiolabeled streptavidin leads to visualization of the remaining biotinylated annexin V at the cell death target site. Annexin V is known to slowly penetrate into cells; thus, the timing between injection of biotinylated annexin V and radiolabeled streptavidin needs be optimized to ensure that enough annexin V remains on the cell surface to generate a useful target signal.[95,96] Ungethum et al. utilized bioinformatics and protein−protein docking methods to create a structure/function relationship for annexin V internalization.[97] This information led to the production of an annexin V variant that remained on the cell surface of apoptotic cells, and performed better as a cell death pretargeting agent than wild-type annexin V.

Other PS-binding proteins have been labeled with reporter groups to produce promising cell death imaging agents. Synaptotagmin-I is a synaptic vesicle associated membrane protein that contains a C2A and C2B domain, the former of which is responsible for Ca^{2+}-dependent binding to PS. Typically, the C2A domain is expressed and used as a recombinant glutathione-S-transferase (GST) fusion protein. Radiolabeling C2A-GST with ^{99m}Tc or ^{18}F produces imaging probes for visualizing cell death in animal models of myocardial infarction and anticancer treatment.[98−100] These radiolabeling procedures are typically performed through amine chemistry on the ε-amino group of surface lysine residues. There are 14 lysine residues in C2A and 35 in C2A-GST; thus, the labeled probes are expected to be a heterogeneous mixture of molecular species with different binding affinities. C2A variants containing His tags and/or a free cysteine have been developed for efficient and site-specific radiolabeling.[101] Alam and co-workers developed a site-directed mutant of C2A, C2Am, in which a serine residue that is distant from the PS-binding site was replaced with a single cysteine residue (S78C).[102] Flow cytometry showed that the fluorescently labeled C2Am had a 4-fold higher specific binding to cell death than a commercially available fluorescent annexin V, although annexin V labeled more apoptotic and necrotic cells. This lower binding of C2Am to viable cells should lead to lower nonspecific accumulation and higher target to background ratios at sites of cell death.

Lactadherin or MFG-E8, a glycoprotein secreted by macrophages, has a discoidin-type C2 domain that is responsible for stereospecific binding to PS in a Ca^{2+}-independent manner. Yeung et al. generated a genetically encoded biosensor for PS by fusing a green fluorescent protein to the C2 domain of lactadherin.[103] In RAW264.7 cells, GFP-Lact-C2 bound to the

cytosolic leaflet of the plasma membrane, endosomes, and lysosomes, and this binding was dependent on PS and not simply anionic charge. Lactadherin was capable of detecting progressively higher levels of exposed PS on the surface of stored platelets and proved to be effective at visualizing PS-associated morphological changes in platelets.[104] The increased sensitivity for exposed PS has prompted efforts to develop SPECT versions of lactadherin for cell death radioimaging. A ^{99m}Tc-HYNIC-lactadherin conjugate was found to have the same biological properties of lactadherin, and biodistribution studies showed rapid clearance from the blood and accumulation in the liver.[105] Additional in vivo testing of this imaging probe seems warranted.

Because of their relatively large molecular sizes, proteins and antibodies have the intrinsic benefit of high binding affinity and high target selectivity, but imaging performance can be limited by stability problems, undesired organ distribution profiles, slow diffusion rates, and slow blood-pool clearance rates. The latter concern is especially problematic for imaging techniques with radioactive probes that have short half-lives and must be cleared rapidly so high contrast imaging can be achieved before the signal is lost. Compared to proteins, it is much easier to systematically fine-tune the pharmacokinetic properties of small molecules, and it is highly advantageous to develop small molecule imaging probes that exhibit the same targeting capabilities as proteins. With these thoughts in mind, investigators have searched for low-molecular-weight molecules that exhibit high and selective PS-binding affinity. Several research groups have independently employed phage panning technology to find different small peptides (hexamers to decamers) that bind exposed PS with nanomolar dissociation constants. Burtea and co-workers screened an M13 phage display library on PS-coated plates and identified a hexapeptide (LIKKPF) with high PS binding affinity but only modest phosphatidylserine/phosphatidylcholine selectivity.[106] Labeling the peptide with a Gd-diethylene triamine pentacetic acid (DTPA) complex produced a targeted MRI contrast agent that was able to visualize cell death in atherosclerotic plaques and in a liver apoptosis mouse model. In an effort to increase probe sensitivity and alleviate possible in vivo toxicities related to gadolinium conjugates, the same group attached another PS-binding hexapeptide (TLVSSL) to ultrasmall superparamagnetic iron oxide particles (USPIO).[107,108] In vivo MRI showed that peptide USPIO particles were able to detect increased apoptosis in tumors subjected to radiation and different chemotherapeutic regimens and in an animal model of atherosclerosis.[109,110] A second research group independently identified CLSYYPSY as a novel PS-interacting octapeptide.[111] A fluorescein labeled version of this peptide specifically homed to the tumor vasculature and apoptotic tumor cells in xenografts treated with camptothecin. Interestingly, the researchers found that a cyclized form of the peptide exhibited more specific binding to apoptotic cells than the linear form. A third group identified a phage projecting 12-mer peptide (SVSVGMKPSPRP) that selectively bound to PS exposed on red blood cells and apoptotic cells.[112] Most recently, Xiong and colleagues used rational design to identify a PS-binding14-mer peptide that was derived from the PS-binding site within a PS decarboxylase enzyme.[113] Modification of the peptide with a ^{99m}Tc chelating group enhanced PS binding affinity to give a nanomolar dissociation constant, while enabling ex vivo radioimaging of tumor cell death produced by paclitaxel treatment. Significant accumulation of the peptide probe in the liver and kidney likely prevented effective in vivo whole-body SPECT imaging of cell death. Using an alternative, rational design approach, Zheng and co-workers developed a new class of cyclic peptides that mimic the PS-binding domain of lactadherin.[114] These cyclic peptides have micromolar association constants for membrane with exposed PS, and produce selective staining of apoptotic cells in culture.

The group of Smith and co-workers have pursued synthetic zinc dipicolylamine (ZnDPA) coordination complexes as an alternative approach to PS-targeting. The membrane association process utilizes a three-component assembly process where Zn^{2+} ions mediate cooperative association of the dipicolylamine ligand and the anionic headgroup of membrane-bound PS. Functionally, this is similar to the way that Ca^{2+} ions act as cofactors for membrane association of annexin V. Initial work showed that a fluorescein labeled ZnDPA can distinguish dead and dying mammalian cells from healthy cells in cell culture.[115] To enable in vivo imaging of cell death, a synthetic fluorescent near-infrared probe, PSS-794, was developed and shown to target the necrotic foci of tumors in living rodents.[116] The versatility and effectiveness of PSS-794 as an in vivo cell death imaging probe was exemplified in animal models of tissue damage, thymus atrophy, antitumor treatment, and traumatic brain injury.[117−121] Wyffels et al. developed a ^{99m}Tc-HYNIC-ZnDPA probe and a related ^{99m}Tc(CO)$_3$-ZnDPA probe and characterized their potential as SPECT cell death imaging agents using anti-Fas liver apoptosis and myocardial ischemia-reperfusion injury mouse models.[122] Both models showed that the probes targeted cell death; however, selective uptake was low, while significant accumulation occurred in the liver and GI tract. Surman et al. developed a ZnDPA lanthanide complex for visualizing anionic membranes through MRI.[123] Gd-ZnDPA selectively targeted apoptotic cells in culture as measured by both MR relaxation rate and signal intensity, and both parameters were dependent on probe concentration. An earlier approach conjugated ZnDPA containing peptides to a magnetofluorescent nanoparticle for detection of apoptotic cells in culture.[124] Expanding on this molecular design strategy, Oltmanns and co-workers have developed a ^{18}F conjugated Zn-cyclen probe for PET imaging of treated tumors in rodent model.[125] Both radiation and taxol treated tumors had higher levels of Zn-cyclen probe than their nontreated controls; however, most of the probe accumulated in the liver and other organs. Optimization of the pharmacokinetics needs to be resolved before ZnDPA and Zn-cyclen probes can be considered for clinical trials.

In addition to targeting surface exposed PS, it appears that probes targeting surface exposed PE are also effective cell death imaging agents. Duramycin, a 19-amino-acid, disulfide cross-linked peptide that binds to membrane bound PE with high affinity and high selectivity, has been the most studied peptide for PE imaging.[126] Covalent modification of duramycin with HYNIC and ^{99m}Tc enabled SPECT imaging of acute cardiac cell death as early as 10 min after probe injection, while providing a favorable pharmacokinetic profile.[127] In irradiated cells, PE is simultaneously exposed with PS on the cell membrane surface, and this pattern of exposure and colocalization is maintained over time.[128] Furthermore, Stafford and Thorpe used biotin and near-infrared fluorescent versions of duramycin to detect exposed PE on the surface of tumor endothelium.[129] Recently, a member of the CD300 family of receptors, CD300a, was shown to specifically bind to PE and PS exposed on dead and dying cells.[130] Further studies should

look at the utility of a labeled CD300a protein for imaging cell death and/or the tumor endothelium.

Targeting plasma membrane phospholipids has proven to be a successful strategy for imaging cell death; yet, the imaging information that is gained by targeting these biomarkers is somewhat limited. Probes targeting PS and/or PE cannot usually distinguish apoptosis from necrosis since the phospholipids are exposed during both cell death processes. Furthermore, nonapoptotic cells such as activated lymphocytes, tumor endothelial cells, tumor cells, and microvesicles are known to display PS on their cellular surfaces.[131−134]

Cell Surface Exposed Histones. Apoptotic cells are known to be a source of DNA fragments, nucleoprotein complexes, and histones that drive the production of autoantibodies in certain autoimmunity conditions such as lupus. Histones are normally organized into nucleosomes (H2A, H2B, H3, H4) or located on the internucleosomal DNA (histone H1) in mammalian cells. During apoptosis, the histones are released from the cytoplasm and subsequently transported to the plasma membrane where they are accessible for recognition by professional phagocytes.[135] The translocation of histone H1 from the nucleus to the cytoplasm and cell surface occurs in the early stages of apoptosis and is mediated by caspases.[136] With this process in mind, Wang et al. utilized phage display to identify CQRPPR hexapeptide (Apopep-1), which bound to histone H1 exposed on the surface of apoptotic cells.[137] Fluorescently labeled Apopep-1 effectively targeted dead and dying cells within tumor tissue, and probe accumulation increased when tumors were treated with anticancer drugs. The Apopep-1 peptide was also shown to detect dying neurons in a preclinical mouse model of Parkinson's disease.[138]

Other Plasma Membrane Biomarkers. The family of small molecule probes produced by Aposense Inc. appear to be promising detectors of apoptosis in living animals. One of the initial compounds, *N*,*N*′-didansyl-L-cystine (DDC) was shown, using fluorescence microscopy, to accumulate in dead and dying cells in a rodent stroke model.[139] Autoradiography using ^{3}H-DDC corroborated the fluorescence results by showing accumulation in the ischemic regions of the brain. Ex vivo fluorescence microscopy of histological samples showed DDC staining of damaged tissue from traumatic brain injury and chemotherapy-induced enteropathy.[140,141] The DDC is proposed to selectively accumulate inside apoptotic cells due to plasma membrane depolarization and activation of scramblase proteins on the cell membrane. A technical drawback with this fluorescent probe is the short wavelength, dansyl fluorophore, which is not highly suitable for cell microscopy or animal imaging. Another dansyl derivative, DFNSH, has also been shown to accumulate in the cytoplasm of dead and dying cancer cells.[142] Radiolabeling of this dansylhydrazone with ^{18}F enabled visualization of ketamine-induced neurotoxicity in rat brains via PET imaging.[143] Aposense Inc. has developed ML-10 as another low-molecular-weight detector of cell death based on the alkyl-malonate group from γ-carboxyglutamic acid. ML-10 showed intracellular uptake in apoptotic cells and did not accumulate in cells where the membrane had been disrupted; thus, the probe could be used to identify cells in early-stage apoptosis.[144] The mechanism of ML-10 uptake is hypothesized to be the result of membrane depolarization and acidification during early apoptosis. To facilitate PET imaging of apoptosis, ML-10 was radiolabeled with^{18}F.[145] In a experimental cerebral stroke mouse model, ^{18}F-ML-10 had a 2-fold higher uptake in the affected cerebral hemisphere and a 6- to 10-fold higher uptake in the region of the infarct, which was validated by histological evidence of cell death. These results prompted a clinical study evaluating the dosimetry, biodistribution, stability, and safety profile of ^{18}F-ML-10 in healthy humans.[146] Administration of ^{18}F-ML-10 appeared to be safe and the probe exhibited high in vivo stability. Most recently, ^{18}F-ML-10 was shown to enable early assessment of brain metastases response in a cohort of 10 oncology patients given whole-body radiation therapy (Figure 5).[147] Overall, ^{18}F-ML-10 appears to be a very promising cell death imaging probe for clinical use in humans. However, it is worth noting that a radioiodinated version of ML-10 was not useful for apoptosis imaging.[148] This suggests that the cell targeting mechanism for this probe family needs to be fully elucidated so that the probe structure can be rationally modified for specific apoptosis imaging applications.

■ NECROSIS BIOMARKERS

Necrosis is often classified as an uncontrolled, accidental process that occurs as the result of physical or chemical insult. However, under certain circumstances a programmed form of necrosis can occur, termed necroptosis. Furthermore, in the absence of efficient cell removal by the immune system, late stage apoptotic cells will subsequently undergo secondary necrosis. Primary and secondary necrosis differ in the time taken for rupture of the plasma membrane and release of intracellular molecules into the extracellular environment. The released molecules, along with changes in intracellular metabolism, can be targeted as biomarkers for necrosis imaging.[149] However, it must be remembered that many biomarkers, like PS exposure, are common to both apoptosis and necrosis and additional imaging data is needed to distinguish them.

A common biomarker for necrosis is the intracellular DNA that becomes accessible after disruption of the cell plasma membrane. Propidium iodide, a fluorescent DNA binding dye, is routinely used in flow cytometry as a secondary marker for necrosis. There appears to be no published studies using this dye for whole-body in vivo necrosis imaging; however, laboratories have used other DNA binding molecules to target necrosis in living animals. Dasari et al. developed a fluorescent necrosis probe by conjugating a near-infrared IR-786 dye to Hoechst, a biocompatible DNA binding agent.[150] The Hoechst-IR probe was shown to distinguish viable cells from dead and dying cells with permeable membranes. When evaluated in necrosis-inducing myocardial infarction and sepsis in vivo models, Hoechst-IR allowed whole-body fluorescence imaging of necrotic tissue. Garanger et al. synthesized a multimodal DNA-binding agent by appending a gadolinium chelating DTPA to TO-PRO-1, which binds to DNA though electrostatic interactions with the phosphate backbone.[151] The Gd-TO probe did not accumulate in viable cells, but showed increased T_1 relaxivity and fluorescence intensity in camptothecin treated cells. The utility of Gd-TO for in vivo necrosis imaging was tested in a permanent myocardial infarction mouse model.[152] Gd-TO allowed visualization of acute necrosis as well as the progression and clearance of necrotic cells from the ischemic myocardium. It is likely that other necrosis imaging probes can be produced using this general strategy of conjugating an imaging contrast agent to a DNA binding molecule, although it is possible that they may suffer from toxicity problems.[153]

A number of other molecular probes with high avidity for necrotic tissue have been used for noninvasive imaging of ischemic myocardial injury, brain infarct, and assessment of

radiofrequency ablation therapies. The most studied of these compounds is hypericin, which is a nonporphyrin photosynthesizer derived from the plant genus *Hypericum*. A radiolabeled derivative of hypericin, mono^{123}I-iodohypericin, allowed visualization of necrotic liver tissue after systematic injection.[154] A less lipophilic version of mono^{123}I-iodohypericin, containing a carboxylic acid, was reported to exhibit faster blood clearance and be better suited for whole-body imaging of necrosis.[155] Pretargeting strategies using biotinylated hypericin and ^{123}I-avidin have been applied for necrotic tumor imaging; however, a problem was poor penetration of the ^{123}I-avidin into necrotic tissue.[156] The inherent fluorescence properties of hypercin have also been exploited for microscopic necrosis imaging.[157,158] Recently, a ^{64}Cu-bis-DOTA-hypericin was used to assess antitumor therapeutic efficacy induced by photothermal ablation.[159] SPECT and PET derivatives of pamoic acid have been used in vivo and ex vivo to delineate necrotic tissue from viable tissue.[160,161] The targeting mechanisms for these compounds and other necrosis probes are not well-known, and may vary with molecular structure.[162,163]

Much attention has been focused on developing biomarkers for necroptosis imaging since it has an important role in numerous biological and pathophysiological settings.[164] Necroptosis can be initiated by the same signaling ligands as apoptosis, though its morphological features are characteristic of pathological necrosis, and it is highly dependent on the activation of receptor-interacting protein-1 (RIP-1) and/or receptor-interacting protein-3 (RIP-3).[165,166] Downstream events of RIP-1 and RIP-3 activation include cytosolic ATP depletion, ROS overproduction, activation of calpains and cathepsins, and lysosomal membrane permeabilization.[164] Currently, only a few of these biomarkers have been investigated as molecular imaging targets. For example, Vanden Berghe et al. utilized a commercially available ROS indicator (CM-H_2DCFDA), a mitochondrial transmembrane potential probe (TMRM), and a lysosome imaging agent (LysoTracker Red DND-99) to investigate the occurrence of necrosis signaling events via live-cell fluorescence imaging.[167] It is worth noting that cathepsin B is one of the enzymes that is released and activated during lysosomal membrane permeabilization, and that cathepsin B activatable fluorescent probes, Cat B 680 FAST and Cat B 750 FAST, are commercially available from Perkin-Elmer. These probes have been validated for whole-body imaging in animal models of cancer [168] and inflammatory-related diseases;[169] however, they have not yet been evaluated in cell death animal models. Cathepsin B inhibitors, such as CA-074 methyl ester, may also be effective for visualizing cell death when labeled with a reporter group.[170] An enzymatic inhibitor of RIP-1 kinase, necrostatin-1, has been discovered to protect against necroptotic cell death both in vitro and in vivo.[171,172] This suggests that necrostatin-1 and other necrostatins may be effective molecular scaffolds for the development of imaging agents that are specific for necroptosis. As stated previously, differentiating cell death pathways can be quite challenging and typically requires careful monitoring of the temporal changes in biomarkers.[173]

■ AUTOPHAGY BIOMARKERS

Autophagy is a programmed biological process where cytoplasmic structures are degraded in lysosomes. At present, autophagy can be divided into three forms, macroautophagy, microautophagy, and chaperone-mediated autophagy, with macroautophagy as the most-extensively studied. Macroautophagy is mediated by special double-membrane vesicles called autophagosomes, which engulf cytoplasmic constituents and deliver them to lysosomes for degradation. Macromolecules generated from the lysosomal degradation are then delivered to the cytosol and reused for energetic or biosynthetic processes.

The initiation and regulation of autophagy relies on a set of Atg proteins that are required for the formation of the autophagosome. The Atg proteins are conserved among highly distant species including yeast and humans. The microtubule-associated protein light chain 3 (LC3), a mammalian homologue of yeast Atg8, is known to exist on autophagosomes, thus it has served as a molecular marker for autophagosomes and subsequently autophagy.[174] Tagging LC3 with a green fluorescent protein has proven to be an effective technique for visualizing and quantifying punctate intracellular structures in living cells and in different model organisms including mice and *Drosophila*. Imaging in larger organisms requires excision of target tissues followed by fixation for fluorescence microscopy. While this technique is useful for evaluating the number of autophagosomes, it may not always be an indicator of autophagic activity. The accumulation of LC3-positive autophagosomes may be the result of increased initiation of autophagy or decreased autophagic degradation, caused by defects in lysosomal fusion or degradation.[173] Studies using static imaging techniques should always include autophagic flux measurements that can discriminate between efficient and arrested autophagy. The various methods to assess autophagy have been discussed in recent review articles.[174,175]

A point of current debate is whether cell death is mediated by autophagy (autophagic cell death) or occurs along with autophagy. In most cases, autophagy plays a cytoprotective role in response to cellular stress. However, there are reports of systems where autophagy appears to be responsible for cell death.[176,177] Factors that make it difficult to assess the contribution of autophagy to cell death, include (a) misdiagnosis of autophagy, (b) increased number of autophagosomes might represent increased initiation or decreased autophagy, (c) lack of specific inhibitors for autophagy, (d) autophagy inhibition may result in changes in morphology or rate of dead cell degradation, and (e) quantitative discrepancy between the magnitude of autophagy inhibition and cell death inhibition.[178] The molecular connections between autophagy and cell death are complex and poorly understood; thus, researchers have proposed criteria that must be met in order to use the term "autophagic cell death". These include (a) prevention of cell death by inhibition of the autophagic pathway by chemical and/or genetic means and (b) increase in autophagic flux, not just an increase in autophagy markers.[179] Studies involving the inhibition or deletion of multiple Atg genes could delineate whether autophagy is mediating cell death in a specific biological context. Understanding the interplay between autophagy and cell death processes could facilitate the development of drugs that manipulate autophagy in cancer and other diseases.

■ UNEXPLORED CELL DEATH BIOMARKERS

While a wide variety of molecular imaging agents show avidity for dead and dying cells and tissue, there are additional biomarkers that could be exploited as whole-body cell death imaging probes. One example is High Mobility Group Box 1 (HMGB1), which is a nonhistone nuclear protein that is passively released into the extracellular environment during

primary and secondary necrosis.[180] When released, HMGB1 acts as a signaling molecule that can interact with a number of pattern recognition receptors, producing a pro-inflammatory environment.[181] HMGB1 levels are elevated in both mouse models and clinical patient samples, and therapeutic intervention with HMGB1 specific antibodies has been shown to rescue mice from lethal sepsis.[182] Additionally, an anti-HMGB1 monoclonal antibody effectively reduced blood-brain-barrier disruption and inhibited brain edema during ischemic insult.[183] Antibodies are commonly used for whole-body imaging for cancer and other disease states, thus it may be feasible to develop a suitably labeled anti-HMGB1 antibody for necrosis imaging.

The surface exposure of calreticulin (ecto-CRT) has been found to be an important signal for the induction of an immunogenic cell death response. Calreticulin is a Ca^{2+}-binding protein that is largely found in the lumen of the endoplasmic reticulum and has been implicated in many diverse functions from regulation of calcium metabolism to cellular adhesion.[184] Upon treatment with anthracyclines or ionizing radiation, cancer cells undergo immunogenic apoptosis where calreticulin is transported to the surface of the cell from the lumen of the ER.[185] The ecto-CRT precedes the exposure of PS and other morphological features of apoptosis and associates with PS at later stages of apoptosis.[186,187] Recently, Jung and co-workers used a fluorescently labeled anti-CRT mAb to noninvasively monitor immunogenic cell death during antitumor treatment.[188] While these results are promising, careful consideration should be used when selecting CRT as a biomarker for cell death. Ecto-CRT can be found on a subset of cells that are not undergoing immunogenic apoptosis including erythrocytes and immune cells.[186,189] Moreover, not all chemotherapeutic agents induce calreticulin exposure on the surface of cells.[185]

Senescence represents a cellular stress response that leads to irreversible cell arrest, which can be induced to counteract disease initiation.[190] A number of characteristics aid in the identification of senescence such as activation of key effector pathways, morphological changes, loss of proliferation, senescence-associated heterochromatic foci production and increased expression of cell cycle inhibitors ($p16^{INK4A}$, $p15^{INK4B}$, p21, and p53).[191,192] The most widely used biomarker for identifying senescence is senescence-associated β-galactosidase (SA-βgal) activity, which is derived from lysosomal β-galactosidase. Both chromogenic and fluorogenic substrates have proven useful for detecting SA-βgal activity in cell culture, excised tissue, and histological sections; however, their in vivo utility remains unknown.[193,194] A number of β-galactosidase substrates have been developed and validated for reporting gene expression in vivo using optical,[195,196] radionuclear,[197] and MR imaging modalities.[198] Recently, a ^{18}F-labeled antisense oligonucleotide was evaluated in vitro for its ability to measure alterations in p21 expression due to cellular irradiation.[199] To our knowledge, these imaging substrates have not been evaluated in animal models of senescence. When conducting imaging studies to identify senescence, more than one biomarker should be targeted since a single marker cannot indisputably identify a senescent cell in vitro and in vivo.[191] Moreover, the choice of biomarkers will likely depend on the disease state and the model system of interest.

THERAPEUTIC STRATEGIES USING CELL DEATH BIOMARKERS

In addition to molecular imaging, cell death biomarkers are potential targets for therapeutic treatments. PS on the cell surface of apoptotic cells acts as an "eat-me" signal for the mononuclear phagocyte system.[200] Generally, macrophages will quickly ingest the apoptotic cells and release an anti-inflammatory response, which can promote tumor growth when apoptotic tumor cells are ingested. If the apoptotic cells are not efficiently cleared by the body, then they can enter secondary necrosis. During secondary necrosis, the plasma membrane becomes irreversibly permeable causing the release of damage associated molecular patterns such as HMGB1, heat shock proteins, SAP130, and so forth.[181] The release of damage associated molecular patterns allows dendritic cells to take up antigens from dead cells, in addition to inducing a costimulatory effect toward these cells. These antigens can promote a specific immune response against apoptotic and necrotic cells. Thus, it is advantageous to shift the clearance of dead and dying cells from macrophages to dendritic cells when developing treatments against cancer and other diseases. Munoz et al. used annexin V to determine if blocking PS could make apoptotic cells immunogenic in vivo.[201] They found that annexin V inhibited cell phagocytosis by monocyte-derived macrophages, thus causing a change in the immunogenicity of apoptotic and necrotic cells. When incubated with irradiated, apoptotic tumor cells, annexin V partially blocked the cell clearance from macrophages causing the tumor cells to undergo secondary necrosis and be taken up by dendritic cells.[202] The presence of annexin V with irradiated tumor cells promoted a pro-inflammatory environment. Challenging lymphoma tumor bearing mice with annexin V and irradiated tumor cells led to inhibition of tumor growth in 60% of mice, whereas irradiated tumor cells alone only stopped growth in 5% of mice. Interestingly, vaccination with annexin V alone caused a reduction in colorectal tumor growth suggesting that molecular targeting of PS in and around the tumor may induce tumor cell death. Indeed, antibodies that specifically bind to PS exposed on the stressed tumor endothelium have been shown to suppress tumor growth in multiple tumor types.[203−205] In addition, mutants of MFG-E8, a bridging molecule that promotes phagocytosis by targeting PS on apoptotic cells and integrins on phagocytes, have been shown to have immunomodulatory properties.[206] Taken together, molecular targeting of PS on stressed and apoptotic cells may be an effective strategy for initiating a pro-inflammatory milieu and suppressing tumor growth.

Histone H1 is an alternative molecular marker of apoptotic cells that can be targeted for drug delivery into tumors. During chemotherapy, tumor cells typically undergo apoptosis, which subsequently increases the levels of cell surface apoptosis biomarkers such as histone H1 and PS. Wang et al. demonstrated an interesting theranostic strategy by preparing doxorubicin-loaded liposomes that were labeled with the histone H1 targeting peptide, Apopep-1.[207] The strategy is summarized schematically in Figure 6. After dosing, the liposomes target the sites of endogenous cell death within a tumor, and if the tumor is responsive to the drug, more cell death occurs. Thus, with every additional treatment, the level of cell death biomarker in the tumor increases and enhances tumor drug delivery. Using a lung tumor xenograft mouse model, the researchers showed that histone-targeted liposomes

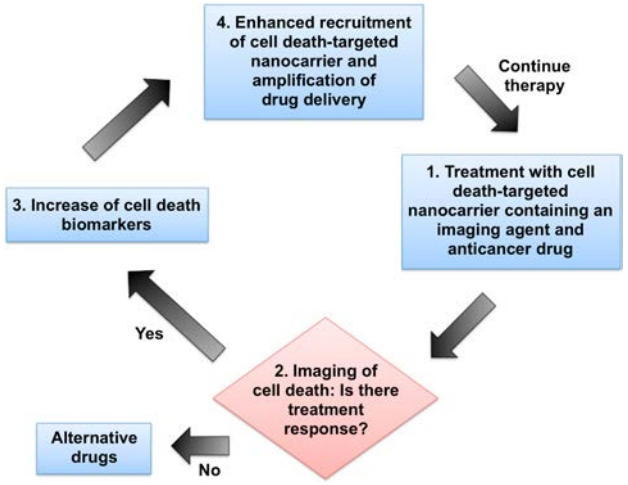

Figure 6. Theranostic strategy using a cell death-targeted drug delivery agent that also monitors treatment response. Adapted from ref 207.

(Apopep-1-DOX) inhibited tumor growth better than folate-targeted and untargeted liposomes. Histone-targeted liposomes that were loaded with a near-infrared dye instead of doxorubicin had higher accumulation in Apopep-1-DOX treated tumors than tumors treated with untargeted liposomes suggesting that these nanoparticles could be used to monitor treatment response. The most recent refinement of this histone-targeted strategy is a cancer immunotherapy study that labeled the surface of T cells with Apopep-1 and found enhanced homing of the cells to doxorubicin-treated tumor.[208] This apoptosis-targeted drug and cell delivery strategy may be applicable to other cell death biomarkers, especially those exposed on the cell surface such as PS. Another possibility is to target the biomarkers that induce senescence.[209,210]

Instead of inducing cell death, there is growing interest in the opposite chemotherapeutic effect of inhibiting cell death. This strategy should be useful for treating diseases associated with excessive cell death such as neurodegenerative diseases, sepsis, cardiovascular diseases, and ischemic injuries.[211,212] Inhibition of caspases during stroke, cardiovascular diseases, and liver failure has proven to be efficacious, and a few caspase inhibitors have entered clinical trials.[213] Recently, Huang and co-workers showed that activated caspase-3 in dying tumor cells can stimulate cell proliferation through the release of soluble lipid messengers, suggesting that caspase inhibitors may also be useful in combination with other chemotherapeutics to prevent tumor recurrence.[214] Researchers have also targeted other biomarkers in the apoptosis pathway. Becattini and co-workers designed a small molecule capable of inhibiting the proapoptotic protein, Bid.[215] An alternative approach delivers the antiapoptotic peptides, Bcl-x_L and BH4, into cells and decreases apoptosis in animal models of sepsis, total-body irradiation, and stroke.[216−218] Pharmacological modulation of nonapoptotic cell death pathways is another strategy for rescuing dead and dying tissues from pathological diseases. Necrostatin-1, a potent inhibitor of necroptosis, decreases injury and improves functional outcome in mouse models of traumatic brain injury, hypoxic-ischemic injury, and Huntington's disease.[219−221] In principle, all of these cell death inhibition strategies could be improved by using in vivo drug delivery strategies that selectively deliver the chemotherapeutic agent to the appropriate anatomical sites undergoing cell death.

CLINICAL IMAGING OF CELL DEATH: CURRENT CHALLENGES AND LIKELY REWARDS

While there has been considerable progress over the last five years, in vivo cell death imaging remains one of the most important unsolved problems in clinical molecular imaging. To be successful in the clinic, many technical challenges must be overcome. First, imaging probes need to accurately detect the spatial and temporal occurrence of specific cell death processes. Diseased tissues such as cancerous tumors are highly heterogeneous and these different cell types can respond differently to treatment. Knowing which cells are undergoing cell death during treatment and where they are located within the tumor will help increase treatment efficacy. The time course for cell death will likely vary with the type of treatment and individual patient response. Currently, cancer therapeutics are assessed using RECIST (Response Evaluation Criteria in Solid Tumors) which is based on measurements of tumor size and is susceptible to incorrect conclusions.[222] The clinical standard of care can likely be improved by incorporating robust molecular imaging methods that evaluate tumor response.[223,224] In other disease areas, the pharmacological challenges for successful cell death imaging are different. For example, neurological disorders require imaging probes that can cross the blood brain barrier. Image contrast will be determined by multiple factors, including the rate of probe clearance from the bloodstream, the rate and location of the cell death process, and the rate of dead cell clearance by the innate immune response. Thus, successful development of an effective cell death imaging probe requires the global optimization of a set of interdependent probe properties (Figure 3). For continued progress toward clinical imaging, structurally well-defined probe candidates must be produced in a cost-effective manner and tested in validated cell death animal models that mimic the genotypic and phenotypic traits seen in humans. The development of clinical methods for simultaneous imaging of cell death and other related physiological processes (metabolism, proliferation, angiogenesis)[13,14] will greatly help clinicians diagnose diseases and make better decisions about personalized treatment options.

AUTHOR INFORMATION

Corresponding Author

*E-mail: smith.115@nd.edu, ph: +1 (574) 631 8632, fax: +1 (574) 631 6652.

Notes

The authors declare no competing financial interest.

ACKNOWLEDGMENTS

We are grateful for funding support from NIH grants R01GM059078 (B.D.S.) and T32GM075762 (B.A.S.).

REFERENCES

(1) Vaux, D. L., and Korsmeyer, S. J. (1999) Cell death in development. *Cell 96*, 245−254.

(2) Thompson, C. B. (1995) Apoptosis in the pathogenesis and treatment of disease. *Science 267*, 1456−1462.

(3) van Heerde, W. L., Robert-Offerman, S., Dumont, E., Hofstra, L., Doevendans, P. A., Smits, J. F. M., Daemen, M. J. A. P., and Reutelingsperger, C. (2000) Markers of apoptosis in cardiovascular tissues: focus on annexin V. *Cardiovasc. Res. 45*, 549−559.

(4) Okada, H., and Mak, T. W. (2004) Pathways of apoptotic and non-apoptotic death in tumor cells. *Nat. Rev. Cancer 4*, 592−603.

(5) Brown, J. M., and Attardi, L. D. (2005) The role of apoptosis in cancer development and treatment response. *Nat. Rev. Cancer 5*, 231−237.
(6) Marx, J. (2006) Autophagy: is it cancer's friend or foe? *Science 312*, 1160−1161.
(7) Blum, E. S., Abraham, M. C., Yoshimura, S., Lu, Y., and Shaham, S. (2012) Control of nonapoptotic developmental cell death in *Carnorhabditis elegans* by a polyglutamine-repeat protein. *Science 335*, 970−973.
(8) Dixon, S. J., Lemberg, K. M., Lamprecht, M. R., Skouta, R., Zaitsev, E. M., Gleason, C. E., Patel, D. N., Bauer, A. J., Cantley, A. M., Yang, W. S., Morrison, B., III, and Stockwell, B. R. (2012) Ferroptosis: an iron-dependent form of nonapoptotic cell death. *Cell 149*, 1060−1072.
(9) Krysko, O., de Ridder, L., and Cornelissen, M. (2004) Phosphatidylserine exposure during early primary necrosis (oncosis) in JB6 cells as evidenced by immunogold labeling technique. *Apoptosis 9*, 495−500.
(10) Festjens, N., Vanden Berghe, T., and Vandenabeele, P. (2006) Necrosis, a well-orchestrated form of cell demise: signaling cascades, important mediators and concomitant immune response. *Biochim. Biophys. Acta 1757*, 1371−1378.
(11) Galluzzi, L., Maiuri, M. C., Vitale, I., Zischka, H., Castedo, M., Zitvogel, L., and Kroemer, G. (2007) Cell death modalities: classification and pathophysiological implications. *Cell Death Differ. 12*, 1237−1266.
(12) Maiuri, M. C., Zalckvar, E., Kimchi, A., and Kroemer, G. (2007) Self-eating and self-killing: crosstalk between autophagy and apoptosis. *Nat. Rev. Mol. Cell Biol. 8*, 741−752.
(13) Plathow, C., and Weber, W. A. (2008) Tumor cell metabolism imaging. *J. Nucl. Med. 49*, 43S−63S.
(14) Salskov, A., Tammisetti, V. S., Grierson, J., and Vesselle, H. (2007) FLT: measuring tumor cell proliferation in vivo with positron emission tomography and 3′-deoxy-3′-[^{18}F]fluorothymidine. *Semin. Nucl. Med. 37*, 429−439.
(15) Lahorte, C. M. M., Vanderheyden, J. L., Steinmetz, N., Van de Wiele, C., Dierckx, R. A., and Slegers, G. (2004) Apoptosis-detecting radioligands: current state of the art and future perspectives. *Eur. J. Nucl. Med. Mol. Imaging 31*, 887−919.
(16) Boersma, H. H., Kietselaer, B. L., Stolk, L. M., Bennaghmouch, A., Hofstra, L., Narula, J., Heidendal, G. A. K., and Reutelingsperger, C. P. (2005) Past, present, and future of Annexin A5: from protein discovery to clinical applications. *J. Nucl. Med. 46*, 2035−2050.
(17) Blankenberg, F. G. (2008) In vivo detection of apoptosis. *J. Nucl. Med. 49*, 81S−95S.
(18) Smith, G., Nguyen, Q. D., and Aboagye, E. O. (2009) Translational imaging of apoptosis. *Anti-Cancer Agent. Med. Chem. 9*, 958−967.
(19) Zhao, M. (2009) In vivo apoptosis imaging agents and strategies. *Anti-Cancer Agent. Med. Chem. 9*, 1018−1023.
(20) Faust, A., Herman, S., Wagner, S., Haufe, G., Schober, O., Schäfers, M., and Kopka, K. (2009) Molecular imaging of apoptosis in vivo with scintigraphic and optical biomarkers − a status report. *Anti-Cancer Agent. Med. Chem. 9*, 968−985.
(21) James, M. L., and Gambhir, S. S. (2012) A molecular imaging primer: modalities, imaging agents, and applications. *Physiol. Rev. 92*, 897−965.
(22) Rao, J., Dragulescu-Andrasi, A., and Yao, H. (2007) Fluorescence imaging in vivo: recent advances. *Curr. Opin. Biotechnol. 18*, 17−25.
(23) Keyaerts, M., Caveliers, V., and Lahouette, T. (2012) Bioluminescence imaging: looking beyond the light. *Trends Mol. Med. 18*, 164−172.
(24) Leblond, F., Davis, S. C., Valdés, P. A., and Pogue, B. W. (2010) Pre-clinical whole-body fluorescence imaging: review of instruments, methods and applications. *J. Photochem. Photobiol. B 98*, 77−94.
(25) Willmann, J. K., van Bruggen, N., Dinkelborg, L. M., and Gambhir, S. S. (2008) Molecular imaging in drug development. *Nat. Rev. Drug Discovery 7*, 591−607.
(26) Sosnovik, D. E., and Weissleder, R. (2007) Emerging concepts in molecular MRI. *Curr. Opin. Biotechnol. 18*, 4−10.
(27) Li, J., and Yuan, J. (2008) Caspases in apoptosis and beyond. *Oncogene 27*, 6194−6206.
(28) Pop, C., and Salvesen, G. S. (2009) Human caspases: activation, specificity, and regulation. *J. Biol. Chem. 284*, 21777−21781.
(29) Fuentes-Prior, P., and Salvesen, G. S. (2004) The protein structures that shape caspase activity, specificity, activation and inhibition. *Biochem. J. 384*, 201−232.
(30) Debunne, M., aPortal, C., Delest, B., Brakenhielm, E., Lallemand, F., Henry, J. P., Ligeret, H., Noack, P., Massonneau, M., Romieu, A., Renard, P. Y., Thuillez, C., and Richard, V. (2011) In vitro and ex vivo evaluation of smart infra-red fluorescent caspase-3 probes for molecular imaging of cardiovascular apoptosis. *Int. J. Mol. Imaging*, DOI: 10.1155/2011/413290.
(31) Joseph, J., Seervi, M., Sobhan, P. K., and Retnabai, S. T. (2011) High throughput ratio imaging to profile caspase activity: potential application in multiparameter high content apoptosis analysis and drug screening. *PLOS One 6*, e20114.
(32) Keese, M., Yagublu, V., Schwenke, K., Post, S., and Bastiaens, P. (2010) Fluorescence lifetime imaging microscopy of chemotherapy-induced apoptosis resistance in a syngenic mouse tumor model. *Int. J. Cancer 126*, 104−113.
(33) Zhang, Z., Fan, J., Cheney, P. P., Berezin, M. Y., Edwards, W. B., Akers, W. J., Shen, D., Liang, K., Culver, J. P., and Achilefu, S. (2009) Activatable molecular systems using homologous near-infrared fluorescent probes for monitoring enzyme activities in vitro, in cellulo, and in vivo. *Mol. Pharmaceutics 6*, 416−427.
(34) Bullock, K. E., Maxwell, D., Kesarwala, A. H., Gammon, S., Prior, J. L., Snow, M., Stanley, S., and Piwnica-Worms, D. (2007) Biochemical and in vivo characterization of a small, membrane-permeant, caspase-activatable far-red fluorescent peptide for imaging apoptosis. *Biochemistry 46*, 4055−4065.
(35) Barnett, E. M., Zhang, X., Maxwell, D., Chang, Q., and Piwnica-Worms, D. (2009) Single-cell imaging of retinal ganglion cell apoptosis with a cell-penetrating, activatable peptide probe in an in vivo glaucoma model. *Proc. Natl. Acad. Sci. U.S.A. 106*, 9391−9396.
(36) Maxwell, D., Chang, Q., Zhang, X., Barnett, E. M., and Piwnica-Worms, D. (2009) An improved cell-penetrating, caspase-activatable, near-infrared fluorescent peptide for apoptosis imaging. *Bioconjugate Chem. 20*, 702−709.
(37) Sun, I. C., Lee, S., Koo, H., Kwon, I. C., Choi, K., Ahn, C. H., and Kim, K. (2010) Caspase sensitive gold nanoparticle for apoptosis imaging in live cells. *Bioconjugate Chem. 21*, 1939−1942.
(38) Jun, Y. W., Sheikholeslami, S., Hostetter, D. R., Tajon, C., Craik, C. S., and Alivisatos, A. P. (2009) Continuous imaging of plasmon rulers in live cells reveals early-stage caspase-3 activation at the single-molecule level. *Proc. Natl. Acad. Sci. U.S.A. 106*, 17735−17740.
(39) Lin, S. Y., Chen, N. T., Sun, S. P., Chang, J. C., Wang, Y. C., Yang, C. S., and Lo, L. W. (2010) The protease-mediated nucleus shuttles of subnanometer gold quantum dots for real-time monitoring of apoptotic cell death. *J. Am. Chem. Soc. 132*, 8309−8315.
(40) Cao, C. Y., Chen, Y., Wu, F. Z., Deng, Y., and Liang, G. L. (2011) Caspase-3 controlled assembly of nanoparticles for fluorescence turn on. *Chem. Commun. 47*, 10320−10322.
(41) Huang, H., Swierczewska, M., Choi, K. Y., Zhu, L., Bhirde, A., Park, J., Kim, K., Xie, J., Niu, G., Lee, K. C., Lee, S., and Chen, X. (2012) Multiplex imaging of an intracellular proteolytic cascade by using a broad-spectrum nanoquencher. *Angew. Chem., Int. Ed. 51*, 1625−1630.
(42) Laxman, B., Hall, D. E., Bhojani, M. S., Hamstra, D. A., Chenevert, T. L., Ross, B. D., and Tehemtulla, A. (2002) Noninvasive real-time imaging of apoptosis. *Proc. Natl. Acad. Sci. U.S.A. 99*, 16551−16555.
(43) Gammon, S. T., Villalobos, V. M., Roshal, M., Samrakandi, M., and Piwnica-Worms, D. (2009) Rational design of novel red-shifted BRET pairs: platforms for real-time single-chain protease biosensors. *Biotechnol. Prog. 25*, 559−569.

(44) Kanno, A., Yamanaka, Y., Hirano, H., Umezawa, Y., and Ozawa, T. (2007) Cyclic luciferase for real-time sensing of caspase-3 activities in living animals. *Angew. Chem., Int. Ed. 46*, 7595−7599.
(45) Ray, P., De, A., Patel, M., and Gambhir, S. S. (2008) Monitoring caspase-3 activation with a multimodality imaging sensor in living subjects. *Clin. Cancer Res. 14*, 5801−5809.
(46) Niers, J. M., Kerami, M., Pike, L., Lewandrowski, G., and Tannous, B. A. (2011) Multimodal in vivo imaging and blood monitoring of intrinsic and extrinsic apoptosis. *Mol. Therapy 19*, 1090−1096.
(47) Coppola, J. M., Ross, B. D., and Rehemtulla, A. (2008) Noninvasive imaging of apoptosis and its application in cancer therapeutics. *Clin. Cancer Res. 14*, 2492−2501.
(48) Hickson, J., Achler, S., Klaubert, D., Bouska, J., Ellis, P., Foster, K., Oleksijew, A., Rodriguez, L., Schlessinger, S., Wang, B., and Frost, D. (2010) Noninvasive molecular imaging of apoptosis in vivo using a modified firefly luciferase substrate, Z-DEVD-Aminoluciferin. *Cell Death Differ. 17*, 1003−1010.
(49) Lee, D., Long, S. A., Adams, J. L., Chan, G., Vaidya, K. S., Francis, T. A., Kikly, K., Winkler, J. D., Sung, C. M., Debouck, C., Richardson, S., Levy, M. A., Dewolf, W. E., Jr., Keller, P. M., Tomaszek, T., Head, M. S., Ryan, M. D., Haltiwanger, R. C., Liang, P. H., Janson, C. A., McDevitt, P. J., Johanson, K., Concha, N. O., Chan, W., Abdel-Meguid, S. S., Badger, A. M., Lark, M. W., Nadeau, D. P., Suva, L. J., Gowen, M., and Nuttall, M. E. (2000) Potent and selective nonpeptide inhibitors of caspases 3 and 7 inhibit apoptosis and maintain cell functionality. *J. Biol. Chem. 275*, 16007−16014.
(50) Nguyen, Q. D., Smith, G., Glaser, M., Perumal, M., Årstad, E., and Aboagye, E. O. (2009) Positron emission tomography imaging of drug-induced tumor apoptosis with a caspase-3/7 specific [^{18}F]-labeled isatin sulfonamide. *Proc. Natl. Acad. Sci. U.S.A. 106*, 16375−16380.
(51) Smith, G., Glaser, M., Perumal, M., Nguyen, Q. D., Shan, B., Arstad, E., and Aboagye, E. O. (2008) Design, synthesis, and biological characterization of a caspase 3/7 selective isatin labeled with 2-[^{18}F]Fluroethylazide. *J. Med. Chem. 51*, 8057−8067.
(52) Nguyen, Q. D., Challapalli, A., Smith, G., Fortt, R., and Aboagye, E. O. (2012) Imaging apoptosis with positron emission tomography: 'bench to bedside' development of the caspase-3/7 specific radiotracer [^{18}F]ICMT-11. *Eur. J. Cancer 48*, 432−440.
(53) Zhou, D., Chu, W., Chen, D. L., Wang, Q., Reichert, D. E., Rothfuss, J., D'Avignon, A., Welch, M. J., and Mach, R. H. (2009) [^{18}F]- and [^{11}C]-Labeled N-benzyl-isatin sulfonamide analogues as PET tracers for apoptosis: synthesis, radiolabeling mechanism, and in vivo imaging study of apoptosis in Fas-treated mice using [^{11}C]WC-98. *Org. Biomol. Chem. 7*, 1337−1348.
(54) Chen, D. L., Zhou, D., Chu, W., Herrbrich, P. E., Jones, L. A., Rothfuss, J. M., Engle, J. T., Geraci, M., Welch, M. J., and Mach, R. H. (2009) Comparison of radiolabeled isatin analogs for imaging apoptosis with positron emission tomography. *Nucl. Med. Biol. 36*, 651−658.
(55) Powers, J. C., Asgian, J. L., Ekici, O. D., and James, K. E. (2002) Irreversible inhibitors of serine, cysteine, and threonine proteases. *Chem. Rev. 102*, 4639−4750.
(56) Edgington, L. E., Berger, A. B., Blum, G., Albrow, V. E., Paulick, M. G., Lineberry, N., and Bogyo, M. (2009) Noninvasive optical imaging of apoptosis by caspase-targeted activity-based probes. *Nat. Med. 8*, 967−973.
(57) Launay, S., Hermine, O., Fontenay, M., Kroemer, G., Solary, E., and Garrido, C. (2005) Vital functions for lethal caspases. *Oncogene 24*, 5137−5148.
(58) Fernando, P., Brunette, S., and Megeney, L. A. (2005) Neural stem cell differentiation is dependent upon endogenous Caspase 3 activity. *FASEB J. 19*, 1671−1673.
(59) Yi, C. H., and Yuan, J. (2009) The Jekyll and Hyde functions of caspases. *Dev. Cell 16*, 21−34.
(60) Rozman-Pungerčar, J., Kopitar-Jerala, N., Bogyo, M., Turk, D., Vasiljeva, O., Stefe, I., Vandenabeele, P., Brömme, D., Puizdar, V., Fonović, M., Trstenjak-Prebanda, M., Dolenc, I., Turk, V., and Turk, B. (2003) Inhibition of palpain-like cysteine proteases and legumain by caspase-specific inhibitors: when reaction mechanism is more important than specificity. *Cell Death Differ. 10*, 881−888.
(61) Ly, J. D., Grubb, D. R., and Lawen, A. (2003) The mitochondrial membrane potential ($\Delta\Psi_m$) in apoptosis; an update. *Apoptosis 8*, 115−128.
(62) Ross, M. F., Kelso, G. F., Blaikie, F. H., James, A. M., Cochemé, H. M., Filipovska, A., Da Ros, T., Hurd, T. R., Smith, R. A. J., and Murphy, M. P. (2005) Lipophilic triphenylphosphonium cations as tools in mitchondrial bioenergetics and free radical biology. *Biochemistry (Moscow) 70*, 222−230.
(63) Nguyen, Q. D., and Aboagye, E. O. (2010) Imaging the life and death of tumors in living subjects: preclinical PET imaging of proliferation and apoptosis. *Integr. Biol. 2*, 483−495.
(64) Madar, I., Huang, Y., Ravert, H., Dairymple, S. L., Davidson, N. E., Isaacs, J. T., Dannals, R. F., and Frost, J. J. (2009) Detection and quantification of the evolution dynamics of apoptosis using the PET voltage sensor ^{18}F-fluorobenzyl triphenyl phosphonium. *J. Nucl. Med. 50*, 774−780.
(65) Madar, I., Ravert, H., Neikin, B., Abro, M., Pomper, M., Dannals, R., and Frost, J. J. (2007) Characterization of membrane potential-dependent uptake of the novel PET tracer ^{18}F-fluorobenzyl triphenylphosphonium cation. *Eur. J. Nucl. Med. Mol. Imaging 34*, 2057−2065.
(66) Pace, N. J., Pimental, D. R., and Weerapana, E. (2012) An inhibitor of glutathione S-transferase omega 1 that selectively targets apoptotic cells. *Angew. Chem., Int. Ed. 51*, 8365−8368.
(67) Kenan, D. J., and Keene, J. D. (2004) La gets its wings. *Nat. Struct. Mol. Biol. 11*, 303−305.
(68) Al-Ejeh, F., Darby, J. M., and Brown, M. P. (2007) The La autoantigen is a malignancy-associated cell death target that is induced by DNA-damaging drugs. *Clin. Cancer Res. 13*, 5509s−5518s.
(69) Al-Ejeh, F., Darby, J. M., Pensa, K., Diener, K. R., Hayball, J. D., and Brown, M. P. (2007) In vivo targeting of dead tumor cells in a murine tumor model using a monoclonal antibody specific for the La autoantigen. *Clin. Cancer Res. 13*, 5519s−5527s.
(70) Al-Ejeh, F., Darby, J. M., Tsopelas, C., Smyth, D., Manavis, J., and Brown, M. P. (2009) APOMAB, a La-specific monoclonal antibody, detects the apoptotic tumor response to life-prolonging and DNA-damaging chemotherapy. *PLoS ONE 4*, e4558.
(71) Park, D., Don, A. S., Massamiri, T., Karwa, A., Warner, B., MacDondald, J., Hemenway, C., Naik, A., Kuan, K. T., Dilda, P. J., Wong, J. W., Camphausen, K., Chinen, L., Dyszlewski, M., and Hogg, P. J. (2011) Noninvasive imaging of cell death using an Hsp90 ligand. *J. Am. Chem. Soc. 133*, 2832−2835.
(72) Chekeni, F. B., Elliot, M. R., Sandilos, J. K., Walk, S. F., Kinchen, J. M., Lazarowski, E. R., Armstrong, A. J., Penuela, S., Laird, D. W., Salvesen, G. S., Isakson, B. E., Bayliss, D. A., and Ravichandran, K. S. (2010) Pannexin 1 channels mediate "find-me" signal release and membrane permeability during apoptosis. *Nature 467*, 863−867.
(73) Emoto, K., Toyama-Sorimachi, N., Karasuyama, H., Inoue, K., and Umeda, M. (1997) Exposure of phosphatidylethanolamine on the surface of apoptotic cells. *Exp. Cell Res. 232*, 430−434.
(74) Vangestel, C., Van de Wiele, C., Van Damme, N., Staelens, S., Pauwels, P., Reutelingsperger, C. P., and Peeters, M. J. (2011) ^{99m}Tc-$(CO)_3$ His-Annexin A5Micro-SPECT demonstrates increased cell death by irinotecan during the vascular normalization window caused by bevacizumab. *J. Nucl. Med. 52*, 1786−1794.
(75) Toretsky, J., Levenson, A., Weinberg, I. N., Tait, J. F., Uren, A., and Mease, R. C. (2004) Preparation of F-18 labeled annexin V: a potential PET radiopharmaceutical for imaging cell death. *Nucl. Med. Biol. 31*, 747−752.
(76) Sosnovik, D. E., Garanger, E., Aikawa, E., Nahrendorf, M., Figuiredo, J. L., Dai, G., Reynolds, F., Rosenzweig, A., Weissleder, R., and Josephson, L. (2009) Molecular MRI of cardiomyocyte apoptosis with simultaneous delayed enhancement MRI distinguishes apoptotic and necrotic myocytes in vivo: potential for midmyocardial salvage in acute ischemia. *Circ. Cardiovasc. Imaging 2*, 460−467.
(77) Min, P. K., Lim, S., Kang, S. J., Hong, S. Y., Hwang, K. C., Chung, K. H., Shim, C. Y., Rim, S. J., and Chung, N. (2010) Targeted

ultrasound imaging of apoptosis with annexin A5 microbubbles in acute doxorubicin-induced cardiotoxicity. *J. Cardiovasc. Ultrasound 18*, 91−97.
(78) Ntziachristos, V., Chellenberger, E. A., Ripoll, J., Yessayan, D., Graves, E., Bogdanov, A., Jr., Josephson, L., and Weissleder, R. (2004) Visualization of antitumor treatment by means of fluorescence molecular tomography with an annexin V-Cy5.5 conjugate. *Proc. Natl. Acad. Sci. U.S.A. 101*, 12294−12299.
(79) Kapty, J., Murray, D., and Mercer, J. (2010) Radiotracers for noninvasive molecular imaging of tumor cell death. *Cancer Biother. Radio. 25*, 615−628.
(80) Beekman, C. A. C., Buckle, T., van Leeuwen, A. C., Valdés Olmos, R. A., Verheij, M., Rottenberg, S., and van Leeuwen, F. W. B. (2011) Questioning the value of ^{99m}Tc-HYNIC-Annexin V based response monitoring after docetaxel treatment in a mouse model for hereditary breast cancer. *Appl. Radiat. Isot. 69*, 656−662.
(81) Lederle, W., Arns, S., Rix, A., Gremse, F., Doleschel, D., Schmalijohann, J., Mottaghy, F. M., Kiessling, F., and Palmowski, M. (2011) Failure of annexin-based apoptosis imaging in the assessment of antiangiogenic therapy effects. *EJNMMI Res 1*, 26.
(82) Niu, G., and Chen, X. (2010) Apoptosis imaging: beyond annexin V. *J. Nucl. Med. 51*, 1659−1662.
(83) Demchenko, A. P. (2012) Beyond annexin V: fluorescence response of cellular membranes to apoptosis. *Cytotechnology*, DOI: 10.1007/s10616-012-9481-y.
(84) Kuge, Y., Zhao, S., Takei, T., and Tamaki, N. (2009) Molecular imaging of apoptosis with radio-labeled Annexin A5 focused on the evaluation of tumor response to chemotherapy. *Anti-Cancer Agent. Med. Chem. 9*, 1003−1011.
(85) Loose, D., Vermeersch, H., De Vos, F., Deron, P., Slegers, G., and Van de Wiele, C. (2008) Prognostic value of ^{99m}Tc-HYNIC Annexin-V imaging in squamous cell carcinoma of the head and neck. *Eur. J. Nucl. Med. Mol. Imaging 35*, 47−52.
(86) Fonge, H., de Saint Hubert, M., Vunickx, K., Rattat, D., Nuyts, J., Bormans, G., Ni, Y., Reutelingsperger, C., and Verbruggen, A. (2008) Preliminary in vivo evaluation of a novel ^{99m}Tc-labeled HYNIC-cys-Annexin A5 as an apoptosis imaging agent. *Bioorg. Med. Chem. Lett. 18*, 3794−3798.
(87) Greupink, R., Sio, C. F., Ederveen, A., and Orsel, J. (2009) Evaluation of a ^{99m}Tc-labeled Annexin A5 variant for non-invasive SPECT imaging of cell death in liver, spleen, and prostate. *Pharm. Res. 26*, 2647−2656.
(88) Vangestel, C., Peeters, M., Oltenfreiter, R., D'Asseler, Y., Staelens, S., Van, Steenkiste, M., Philippé, J., Kusters, D., Reutelingsperger, C., Van Damme, N., and Van de Wiele, C. (2010) In vitro and in vivo evaluation of [^{99m}Tc]-labeled tricarbonyl His-Annexin A5 as an imaging agent for the detection of phosphatidylserine-expressing cells. *Nucl. Med. Biol. 37*, 965−975.
(89) Kurihara, H., Yang, D. J., Cristofanilli, M., Erwin, W. D., Yu, D. F., Kohanim, S., Mendez, R., and Kim, E. E. (2008) Imaging and dosimetry of ^{99m}Tc-EC-Annexin V: preliminary clinical study targeting apoptosis in breast tumors. *Appl. Radiat. Isot. 66*, 1175−1182.
(90) Bauwens, M., De Saint-Hubert, M., Devos, E., Deckers, N., Reutelingsperger, C., Mortelmans, L., Himmelreich, U., Mottaghy, F. M., and Verbruggen, A. (2011) Site-specific ^{68}Ga-labeled Annexin A5 as a PET imaging agent for apoptosis. *Nucl. Med. Biol. 38*, 381−392.
(91) Li, X., Link, J. M., Stekhova, S., Yagle, K. J., Smith, C., Krohn, K. A., and Tait, J. F. (2008) Site-specific labeling of annexin V with F-18 for apoptosis imaging. *Bioconjugate Chem. 19*, 1684−1688.
(92) Hu, S., Kiesewetter, D. O., Zhu, L., Guo, N., Gao, H., Liu, G., Hida, N., Lang, L., Niu, G., and Chen, X. (2012) Longitudinal PET imaging of doxorubicin-induced cell death with ^{18}F-Annexin V. *Mol. Imaging Biol.*, DOI: 10.1007/s11307-012-0551-5.
(93) Cheng, Q., Lu, L., Grafström, M. H., Thorell, J. O., Samén, E., Johansson, K., Ahlzén, H. S., Stone-Elander, S., Linder, S., Arnér, E. S. J., and Sel-tag Imaging Project (2012) Combining [^{11}C]-AnxA5 PET imaging with serum biomarkers for improved detection in live mice of modest cell death in human solid tumor xenografts. *PLoS One 7*, e42151.
(94) Cauchon, N., Langlois, R., Rousseau, J. A., Tessier, G., Cadorette, J., Lecomte, R., Hunting, D. J., Pavan, R. A., Zeisler, S. K., and van Lier, J. E. (2007) PET imaging of apoptosis with ^{64}Cu-labeled streptavidin following pretargeting of phosphatidylserine with biotinylated Annexin-V. *Eur. J. Nucl. Med. Mol. Imaging 34*, 247−258.
(95) Kenis, H., van Genderen, H., Bennaghmouchm, A., Rinia, H. A., Frederik, P., Narula, J., Hofstra, L., and Reutelingsperger, C. P. (2004) Cell surface-expressed phosphatidylserine and Annexin A5 open a novel portal of cell entry. *J. Biol. Chem. 279*, 52623−52629.
(96) van Tilborg, G. A., Geelen, T., Duimel, H., Bomans, P. H., Frederik, P. M., Sanders, H. M., Deckers, N. M., Reutelingsperger, C. P., Strijkers, G. J., and Nicolay, K. (2009) Internalization of Annexin A5-functionalized iron oxide particles by apoptotic jurkat cells. *Contr. Media Mol. Imaging 4*, 24−32.
(97) Ungethüm, L., Kenis, H., Nicolaes, G. A., Autin, L., Stoilova-McPhie, S., and Reutelingsperger, C. P. (2011) Engineered Annexin A5 variants have impaired cell entry for molecular imaging of apoptosis using pretargeting strategies. *J. Biol. Chem. 286*, 1903−1910.
(98) Fang, W., Wang, F., Ji, S., Zhu, X., Meier, H. T., Hellman, R. S., Brindle, K. M., Davletov, B., and Zhao, M. (2007) SPECT imaging of myocardial infarction using ^{99m}Tc-labeled C2A domain of Synaptotagmin I in a porcine ischemia-reperfusion model. *Nucl. Med. Biol. 34*, 917−923.
(99) Wang, F., Fang, W., Zhoa, M., Wang, Z., Ji, S., Li, Y., and Zheng, Y. (2008) Imaging Paclitaxel (chemotherapy)-induced tumor apoptosis with ^{99m}Tc C2A, a domain of Synaptotagmin I: a preliminary study. *Nucl. Med. Biol. 35*, 359−364.
(100) Wang, F., Fang, W., Zhang, M. R., Zhao, M., Liu, B., Wang, Z., Hua, Z., Yang, M., Kumata, K., Hatori, A., Yamasaki, T., Yanamoto, K., and Suzuki, K. (2011) Evaluation of chemotherapy response in VX2 rabbit lung cancer with ^{18}F-labeled C2A domain of Synaptotagmin I. *J. Nucl. Med. 52*, 592−599.
(101) Tavaré, R., Torres Martin de Rosales, R., Blower, P. J., and Mullen, G. E. (2009) Efficient site-specific radiolabeling of a modified C2A domain of Synaptotagmin I with $[^{99m}Tc(CO)_3]^+$: a new radiopharmaceutical for imaging cell death. *Bioconjugate Chem. 20*, 2071−2081.
(102) Alam, I. S., Neves, A. A., Witney, T. H., Boren, J., and Brindle, K. M. (2010) Comparison of the C2A domain of Synaptotagmin-I and Annexin-V as probes for detecting cell death. *Bioconjugate Chem. 21*, 884−891.
(103) Yeung, T., Gilbert, G. E., Shi, J., Silvius, J., Kapus, A., and Grinstein, S. (2008) Membrane phosphatidylserine regulates surface charge and protein localization. *Science 319*, 210−213.
(104) Hou, J., Fu, Y., Zhou, J., Li, W., Xie, R., Cao, F., Gilbert, G. E., and Shi, J. (2011) Lactadherin functions as a probe for phosphatidylserine exposure and as an anticoagulant in the study of stored platelets. *Vox Sanguins 100*, 187−195.
(105) Falborg, L., Waehrens., L. N., Alsner, J., Bluhme, H., Frøkiaer, J., Heegaard, C. W., Horseman, M. R., Rasmussen, J. T., and Rehling, M. (2010) Biodistribution of ^{99m}Tc-HYNIC-Lactadherin in mice − a potential tracer for visualizing apoptosis in vivo. *Scand. J. Clin. Lab. Invest. 70*, 209−216.
(106) Burtea, C., Laurent, S., Lancelot, E., Ballet, S., Murariu, O., Rousseaux, O., Port, M., Vander Elst, L., Corot, C., and Muller, R. N. (2009) Peptidic targeting of phosphatidylserine for the MRI detection of apoptosis in atherosclerotic plaques. *Mol. Pharmaceutics 6*, 1903−1919.
(107) Laumonier, C., Segers, J., Laurent, S., Michel, A., Coppée, F., Belayew, A., Vander Elst, L., and Muller, R. N. (2006) A new peptide vector for molecular imaging of apoptosis identified by phage display technology. *J. Biomol. Screen. 11*, 537−545.
(108) Radermacher, K. A., Boutry, S., Laurent, S., Elst, L. V., Mahieu, I., Bouzin, C., Magat, J., Gregoire, V., Feron, O., Muller, R. N., Jordan, B. F., and Gallez, B. (2010) Iron oxide particles covered with hexapeptides targeted at phosphatidylserine as MR biomarkers of tumor cell death. *Contr. Media Mol. Imaging 5*, 258−267.
(109) Radermacher, K. A., Magat, J., Bouzin, C., Laurent, S., Dresselaers, T., Himmelreich, U., Boutry, S., Mahieu, I., Vander Elst,

L., Feron, O., Muller, R. N., Jordan, B. F., and Gallez, B. (2011) Multimodal assessment of early tumor response to chemotherapy: comparison between diffusion-weighted MRI, ^{1}H-MR spectroscopy of choline and USPIO particles targeted at cell death. *NMR Biomed. 25*, 514−522.
(110) Burtea, C., Ballet, S., Laurent, S., Rousseaux, O., Dencausse, A., Gonzalez, W., Port, M., Corot, C., Vander Elst, L., and Muller, R. N. (2012) Development of a magnetic resonance imaging protocol for the characterization of atherosclerotic plaque by using vascular cell adhesion molecule-1 and apoptosis-targeted ultrasmall superparamagnetic iron oxide derivatives. *Arterioscler. Thromb. Vasc. Biol. 32*, e36−348.
(111) Thapa, N., Kim, S., So, I. S., Lee, B. H., Kwon, I. C., Choi, K., and Kim, I. S. (2008) Discovery of a phosphatidylserine-recognizing peptide and its utility in molecular imaging of tumour apoptosis. *J. Cell. Mol. Med. 12*, 1649−1660.
(112) Shao, R., Xiong, C., Wen, X., Gelovani, J. G., and Li, C. (2007) Targeting phosphatidylserine on apoptotic cells with phages and peptides selected from a bacteriophage display library. *Mol. Imaging 6*, 417−426.
(113) Xiong, C., Brewer, K., Song, S., Zhang, R., Lu, W., Wen, X., and Li, C. (2011) Peptide-based imaging agents targeting phosphatidylserine for the detection of apoptosis. *J. Med. Chem. 54*, 1825−1835.
(114) Zheng, H., Wang, F., Wang, Q., and Gao, J. (2011) Cofactor-free detection of phosphatidylserine with cyclic peptides mimicking lactadherin. *J. Am. Chem. Soc. 133*, 15280−15283.
(115) Hanshaw, R. G., Lakshmi, C., Lambert, T. N., and Smith, B. D. (2005) Fluorescent detection of apoptotic cells by using zinc coordination complexes with a selective affinity for membrane surfaces enriched with phosphatidylserine. *ChemBioChem 12*, 2214−2220.
(116) Smith, B. A., Akers, W. J., Leevy, W. M., Lampkins, A. J., Xiao, S., Wolter, W., Suckow, M. A., Achilefu, S., and Smith, B. D. (2010) Optical imaging of mammary and prostate tumors in living animals using a synthetic near infrared zinc(II)-dipicolylamine probe for anionic cell surfaces. *J. Am. Chem. Soc. 132*, 67−69.
(117) Smith, B. A., Gammon, S. T., Xiao, S., Wang, W., Chapman, S., McDermott, R., Suckow, M. A., Johnson, J. R., Piwnica-Worms, D., Gokel, G. W., Smith, B. D., and Leevy, W. M. (2011) In vivo optical imaging of acute cell death using a near-infrared fluorescent zinc-dipicolylamine probe. *Mol. Pharmaceutics 8*, 583−590.
(118) Smith, B. A., Xiao, S., Wolter, W., Wheeler, J., Suckow, M. A., and Smith, B. D. (2011) In vivo targeting of cell death using a synthetic fluorescent molecular probe. *Apoptosis 16*, 722−731.
(119) Smith, B. A., Daschbach, M. M., Gammon, S. T., Xiao, S., Chapman, S. E., Hudson, C., Suckow, M. A., Piwnica-Worms, D., Gokel, G. W., and Leevy, W. M. (2011) In vivo cell death mediated by synthetic ion channels. *Chem. Commun. 47*, 7977−7979.
(120) Hu, S., Chai, W., Liu, Z., Yin, C., and Lei, M. (2011) Near-infrared fluorescent zinc-dipicolylamine: a new molecular imaging probe to monitor the efficiency of chemotherapy. *J. Cent. South Univ. Med. Sci. 36*, 760−764.
(121) Smith, B. A., Xie, B., van Beek, E. R., Que, I., Blankevoort, V., Xiao, S., Cole, E., Hoehn, M., Kaijzel, E. L., Löwik, C. W. G. M., and Smith, B. D. (2012) Multicolor fluorescence imaging of traumatic brain injury in a cryolesion mouse model. *ACS Chem. Neurosci. 3*, 530−537.
(122) Wyffels, L., Gray, B. D., Barber, C., Moore, S. K., Woolfenden, J. M., Pak, K. Y., and Liu, Z. (2011) Synthesis and preliminary evaluation of radiolabeled Bis(Zinc(II)-Dipicolylamine) coordination complexes as cell death imaging agents. *Bioorg. Med. Chem. 19*, 3425−3433.
(123) Surman, A. J., Kenny, G. D., Kumar, D. K., Bell, J. D., Casey, D. R., and Vilar, R. (2011) Targeting of anionic membrane species by lanthanide(III) complexes: towards improved MRI contrast agents for apoptosis. *Chem. Commun. 47*, 10245−10247.
(124) Quinti, L., Weissleder, R., and Tung, C. H. (2006) A fluorescent nanosensor for apoptotic cells. *Nano Lett. 6*, 488−490.
(125) Oltmanns, D., Zitzmann-Kolbe, S., Mueller, A., Bauder-Wuest, U., Schaefer, M., Eder, M., Haberkorn, U., and Eisenhut, M. (2011) Zn(II)-Bis(Cyclen) complexes and the imaging of apoptosis/necrosis. *Bioconjugate Chem. 2011*, 22611−2624.
(126) Zhao, M. (2011) Lantibiotics as probes for phosphatidylethanolamine. *Amino Acids 41*, 1071−1079.
(127) Zhao, M., Li, Z., and Bugenhagen, S. (2008) ^{99m}Tc-Labeled Duramycin as a novel phosphatidylethanolamine-binding molecular probe. *J. Nucl. Med. 49*, 1345−1352.
(128) Marconescu, A., and Thorpe, P. E. (2008) Coincident exposure of phosphatidylethanolamine and anionic phospholipids on the surface of irradiated cells. *Biochim. Biophys. Acta 1778*, 2217−2224.
(129) Stafford, J. H., and Thorpe, P. E. (2011) Increased exposure of phosphatidylethanolamine on the surface of tumor vascular endothelium. *Neoplasia 13*, 299−308.
(130) Simhadri, V. R., Andersen, J. F., Calvo, E., Choi, S. C., Coligan, J. E., and Borrego, F. (2012) Human CD300a binds to phosphatidylethanolamine and phosphatidylserine, and modulates the phagocytosis of dead cells. *Blood 119*, 2799−2809.
(131) Elliot, J. I., Surprenant, A., Marelli-Berg, F. M., Cooper, J. C., Cassady-Cain, R. L., Wooding, C., Linton, K., Alexander, D. R., and Higgins, C. F. (2005) Membrane phosphatidylserine distribution as a non-apoptotic signalling mechanism in lymphocytes. *Nat. Cell Biol. 7*, 808−816.
(132) Ran, S., Downes, A., and Thorpe, P. E. (2002) Increased exposure of anionic phospholipids on the surface of tumor blood vessels. *Cancer Res. 62*, 6132−6140.
(133) Riedl, S., Rinner, B., Asslaber, M., Schaider, H., Walzer, S., Novak, A., Lohner, K., and Zweytick, D. (2011) In search of a novel target − phosphatidylserine exposed by non-apoptotic tumor cells and metastases of malignancies with poor treatment efficacy. *Biochim. Biophys. Acta 1808*, 2638−2645.
(134) Lima, L. G., Chammas, R., Monteiro, R. Q., Moreira, M. E., and Barcinski, M. A. (2009) Tumor-derived microvesicles modulate the establishment of metastatic melanoma in a phosphatidylserine-dependent manner. *Cancer Lett. 283*, 168−175.
(135) Radic, M., Marion, T., and Monestier, M. (2004) Nucleosomes are exposed at the cell surface in apoptosis. *J. Immunol. 172*, 6692−6700.
(136) Ohsawa, S., Hamada, S., Yoshida, H., and Miura, M. (2008) Caspase-mediated changes in Histone H1 in early apoptosis: prolonged caspase activation in devloping olfactory sensory neurons. *Cell Death Differ. 15*, 1429−1439.
(137) Wang, K., Purushotham, S., Lee, J. Y., Na, M. H., Park, H., Oh, S. J., Park, R. W., Park, J. Y., Lee, E., Cho, B. C., Song, M. N., Maek, M. C., Kwak, W., Yoo, J., Hoffman, A. S., Oh, Y. K., Kim, I. S., and Lee, B. H. (2010) In vivo imaging of tumor apoptosis using Histone H1-targeting peptide. *J. Controlled Release 148*, 283−291.
(138) Lee, M. J., Wang, K., Kim, I. S., Lee, B. H., and Han, H. S. (2012) Molecular imaging of cell death in an experimental model of Parkinson's disease with a novel apoptosis-targeting peptide. *Mol. Imaging Biol. 14*, 147−155.
(139) Reshef, A., Shirvan, A., Grimberg, H., Levin, G., Cohen, A., Mayk, A., Kidron, D., Djaldetti, R., Melamed, E., and Ziv, I. (2007) Novel molecular imaging of cell death in experimental cerebral stroke. *Brain Res. 1144*, 156−164.
(140) Reshef, A., Shirvan, A., Shohami, E., Grimberg, H., Levin, G., Cohen, A., Trembovier, V., and Ziv, I. (2008) Targeting cell death in vivo in experimental traumatic brain injury by a novel molecular probe. *J. Neurotrauma 25*, 569−580.
(141) Levin, G., Shirvan, A., Gromberg, H., Reshef, A., Yogev-Falach, M., Cohen, A., and Ziv, I. (2009) Novel fluorescence molecular imaging of chemotherapy-induced intestinal apoptosis. *J. Biomed. Opt. 14*, 054019.
(142) Zeng, W., Yao, M. L., Townsend, D., Kabalka, G., Wall, J., Le Puil, M., Biggerstaff, J., and Miao, W. (2008) Synthesis, biological evaluation and radiochemical labeling of a dansylhydrazone derivative as a potential imaging agent for apoptosis. *Bioorg. Med. Chem. Lett. 18*, 3573−3577.
(143) Zhang, X., Paule, M. G., Newport, G. D., Sadovova, N., Berridge, M. S., Apana, S. M., Kabalka, G., Miao, W., Slikker, W., Jr.,

and Wang, C. (2011) MicroPET imaging of ketamine-induced neuronal apoptosis with radiolabeled DFNSH. *J. Neural Transm. 118*, 203−211.
(144) Cohen, A., Shirvan, A., Levin, G., Grimberg, H., Reshef, A., and Ziv, I. (2009) From the Gla doman to a novel small-molecule detector of apoptosis. *Cell Res. 19*, 625−637.
(145) Reshef, A., Shirvan, A., Waterhouse, R. N., Grimberg, H., Levin, G., Cohen, A., Ulysse, L. G., Friedman, G., Antoni, G., and Ziv, I. (2008) Molecular imaging neurovascular cell death in experimental cerebral stroke by PET. *J. Nucl. Med. 49*, 1520−1528.
(146) Hoglund, J., Shirvan, Antoni, G., Gistavsson, S., Å, Långström, B., Ringheim, A., Sörensen, J., Ben-Ami, M., and Ziv, I. (2011) ^{18}F-ML-10, a PET tracer for apoptosis: first human study. *J. Nucl. Med. 52*, 720−725.
(147) Allen, A. M., Ben-Ami, M., Reshef, A., Steinmetz, A, Kundel, Y., Inbar, E., Djaldetti, R., Davidson, T., Fenig, E., and Ziv, I. (2012) Assessment of response of brain metastases to radiotherapy by PET imaging of apoptosis with ^{18}F-ML-10. *Eur. J. Nucl. Med. Mol. Imaging 39*, 1400−1408.
(148) Bauwens, M., De Saint-Hubert, M., Cleyhens, J., Brams, L., Devos, E., Mottaghy, F. M., and Verbruggen, A. (2012) Radio-iodinated phenylalkyl malonic acid derivatives as pH-sensitive SPECT tracers. *PLoS One 7*, e38428.
(149) Gallagher, F. A., Kettunen, M. I., Hu, D. E., Jensen, P. R., Zandt, R. I., Karlsson, M., Gisselsson, A., Nelson, S. K., Witney, T. H., Bohndiek, S. E., Hansson, G., Peitersen, T., Lerche, M. H., and Brindle, K. M. (2009) Production of hyperpolarized [1,4-$^{13}C_2$]Malate from [1,4-$^{13}C_2$]Fumarate is a marker of cell necrosis and treatment response in tumors. *Proc. Natl. Acad. Sci. U.S.A. 106*, 19801−19806.
(150) Dasari, M., Lee, S., Sy, J., Kim, D., Lee, S., Brown, M., Davis, M., and Murthy, N. (2010) Hoechst-IR: an imaging agent that detects necrotic tissue in vivo by binding extracellular DNA. *Org. Lett. 12*, 3300−3303.
(151) Garanger, E., Hilderbrand, S. A., Blois, J. T., Sosnovik, D. E., Weissleder, R., and Josephson, L. (2009) A DNA-binding Gd chelate for the detection of cell death by MRI. *Chem. Commun. 29*, 4444−4446.
(152) Huang, S., Chen, H. H., Yuan, H., Dai, G., Schuhle, D. T., Mekkaoui, C., Ngoy, S., Liao, R., Caravan, P., Josephson, L., and Sosnovik, D. E. (2011) Molecular MRI of acute necrosis with a novel DNA-binding gadolinium chelate: kinetics of cell death and clearance in infarcted myocardium. *Circ. Cardiovasc. Imaging 4*, 729−737.
(153) Telford, W. G., King, L. E., and Fraker, P. J. (1992) Comparative evaluation of several DNA binding dyes in the detection of apoptosis-associated chromatin degradation by flow cytometry. *Cytometry 13*, 137−143.
(154) Ni, Y., Huyghe, D., Verbeke, K., de Witte, P. A., Nuyts, J., Mortelmans, L., Chen, F., Marchal, G., Verbruggen, A. M., and Bormans, G. M. (2006) First preclinical evaluation of mono-[^{123}I]Iodohypericin as a necrosis-avid tracer agent. *Eur. J. Nucl. Med. Mol. Imaging 33*, 595−601.
(155) Fonge, H., Jin, L., Wang, H., Ni, Y., Bormans, G. M., and Verbruggen, A. M. (2007) Synthesis and preliminary evalulation of mono-[^{123}I]Iodohypericin monocarboxylic acid as a necrosis avid imaging agent. *Bioorg. Med. Chem. Lett. 17*, 4001−4005.
(156) Marysael, T., Bauwens, M., Ni, Y., Bormans, G. M., Rozenski, J., and de Witte, P. A. (2011) Pretargeting of necrotic tumors with biotinylated hypericin using ^{123}I-labeled avidin: evaluation of a two-step strategy. *Invest. New Drugs*, DOI: 10.1007/s10637-011-9778-2.
(157) Wynn, J. L., and Cotton, T. M. (1995) Spectroscopic properties of hypericin in solution and at surface. *J. Phys. Chem. 99*, 4317−4323.
(158) Van de Putte, M., Wang, H., Chen., F., De Witte, P. A., and Ni, Y. (2008) Hypericin as a marker for determination of tissue viability after radiofrequency ablation in a murine liver tumor model. *Oncol. Rep. 19*, 927−932.
(159) Song, S., Xiong, C., Zhou, M., Lu, W., Huang, Q., Ku, G., Zhao, J., Flores, L. G., Jr., Ni, Y., and Li, C. (2011) Small-animal PET of tumor damage induced by photothermal ablation with ^{64}Cu-Bis-DOTA-Hypericin. *J. Nucl. Med. 52*, 792−799.
(160) Fonge, H., Chitneni, S. K., Lixin, J., Vunckx, K., Prinsen, K., Nuyts, J., Mortelmans, L., Bormans, G. M., Ni, Y., and Verbruggen, A. (2007) Necrosis avidity of ^{99m}Tc(CO)$_3$-labeled pamoic acid derivatives: synthesis and preliminary biological evaluation in animal models of necrosis. *Bioconjugate Chem. 18*, 1924−1934.
(161) Prinsen, K., Li, J., Vanbilloen, H., Vermaelen, P., Devos, E., Mortelmans, L., Bormans, G. M., Ni, Y., and Verbruggen, A. (2010) Development and evaluation of a ^{68}Ga labeled pamoic acid derivative for in vivo visualization of necrosis using positron emission tomography. *Bioorg. Med. Chem. Lett. 18*, 5274−5281.
(162) Prinsen, K., Jin, L., Vunckx, K., de Saint-Hubert, M., Zhou, L., Cleynhens, J., Nuyts, J., Bormans, G. M., Ni, Y., and Verbruggen, A. (2011) Radiolabeling and preliminary biological evaluation of a ^{99m}Tc(CO)$_3$ labeled 3,3′-(Benzylidene)-Bis-(^{1}H-Indole-2-Carbohydrazide) derivative as a potential SPECT tracer for in vivo visualization of necrosis. *Bioorg. Med. Chem. Lett. 21*, 502−505.
(163) Van de Putte, M., Ni, Y., and de Witte, P. A. (2008) Exploration of the mechanism underlying the tumor necrosis avidity of hypericin. *Oncol. Rep. 19*, 921−926.
(164) Vandenabeele, P., Galluzzi, L., Vanden Berghe, T., and Kroemer, G. (2010) Molecular mechanisms of necroptosis: an ordered cellular explosion. *Nat. Rev. Mol. Cell Biol. 11*, 700−714.
(165) Degterev, A., and Yuan, J. (2008) Expansion and evolution of cell death programmes. *Nat. Rev. Mol. Cell Biol. 9*, 378−390.
(166) Galluzzi, L., Vitale, I., Abrams, J. M., Alnemri, E. S., Baehrecke, E. H., Blagosklonny, M. V., Dawson, T. M., Dawson, V. L., El-Deiry, W. S., Fulda, S., Gottleib, E., Green, D. R., Hengartner, M. O., Kepp, O., Knight, R. A., Kumar, S., Lipton, S. A., Lu, X., Madeo, F., Malorni, W., Mahlen, P., Nuñez, G., Peter, M. E., Piacentini, M., Rubinsztein, D. C., Shi, Y., Simon, H. U., Vandenabeele, P., White, E., Yuan, J., Zhivotovsky, B., Melino, G., and Kroemer, G. (2012) Molecular definitions of cell death subroutines: recommendations of the nomenclature committee on cell death 2012. *Cell Death Differ. 19*, 107−120.
(167) Vanden Berghe, T., Vanlangenakker, N., Parthoens, E., Deckers, W., Devos, M., Festjens, N., Guerin, C. J., Brunk, U. T., Declercq, W., and Vandenabeele, P. (2010) Necroptosis, necrosis and secondary necrosis converge on similar cellular disintegration features. *Cell Death Differ. 17*, 922−930.
(168) Weissleder, R., Tung, C. H., Mahmood, U., and Bogdanov, A., Jr. (1999) In vivo imaging of tumors with protease-activated near-infrared fluorescent probes. *Nat. Biotechnol. 17*, 375−378.
(169) Jaffer, F. A., Vinegoni, C., John, M. C., Aikawa, E., Gold, H. K., Finn, A. V., Ntziachristos, V., Libby, P., and Weissleder, R. (2008) Real-time catheter molecular sensing of inflammation in proteolytically active atherosclerosis. *Circulation 118*, 1802−1809.
(170) Bröker, L. E., Huisman, C., Span, S. W., Rodriguez, J. A., Kruyt, F. A., and Giaccone, G. (2004) Cathepsin B mediates caspase-independent cell death induced by microtubule stabilizing agents in non-small cell lung cancer cells. *Cancer Res. 64*, 27−30.
(171) Degterev, A., Huang, Z., Boyce, M., Li, Y., Jagtap, P., Mizushima, N., Cuny, G. D., Mitchison, T. J., Moskowitz, M. A., and Yuan, J. (2005) Chemical inhibitor of nonapoptotic cell death with therapeutic potential for ischemic brain injury. *Nat. Chem. Biol. 1*, 112−119.
(172) Degterev, A., Hitomi, J., Germscheid, M., Ch'en, I. L., Korkina, O., Teng, X., Abbott, D., Cuny, G. D., Yuan, C., Wagner, G., Hedrick, S. M., Gerber, S. A., Lugovskoy, A., and Yuan, J. (2008) Identification of RIP1 kinase as a specific cellular target of necrostatins. *Nat. Chem. Biol. 4*, 313−321.
(173) Kepp, O., Galluzzi, L., Lipinski, M., Yuan, J., and Kroemer, G. (2011) Cell death assays for drug discovery. *Nat. Rev. Drug Discovery 10*, 221−236.
(174) Mizushima, N., Yoshimori, T., and Levine, B. (2010) Methods in mammalian autophagy research. *Cell 140*, 313−326.
(175) Klionsky, D. J., Abeliovich, H., Agostinis, P., Agrawal, D. K., Aliev, G., Askew, D. S., Baba, M., Baehrecke, E. H., Bahr, B. A.,

Ballabio, A., Bamber, B. A., Bassham, D. C., Bergamini, E., Bi, X., Biard-Piechaczyk, M., et al. (2008) Guidelines for the use and interpretation of assays for monitoring autophagy in higher eukaryotes. *Autophagy 4*, 151−175.
(176) Fazi, B., Bursch, W., Fimia, G. M., Nardacci, R., Piacentini, M., Di San, F., and Piredda, L. (2008) Fenretinide induces autophagic cell death in caspase-defective breast cancer cells. *Autophagy 4*, 435−441.
(177) Laane, E., Tamm, K. P., Buentke, E., Ito, K., Jharaziha, P., Oscarsson, J., Corcoran, M., Björklund, A. C., Hultenby, K., Lundin, J., Heyman, M., Söderhäll, S., Mazur, J., Porwit, A., Pandolfi, P. P., Zhivotovsky, B., Panaretakis, T., and Grandér, D. (2009) Cell death induced by dexamethasone in lymphoid leukemia is mediated through initiation of autophagy. *Cell Death Differ. 16*, 1018−1029.
(178) Kroemer, G., and Levine, B. (2008) Autophagic cell death: the story of a misnomer. *Nat. Rev. Mol. Cell Biol. 9*, 1004−1010.
(179) Denton, D., Nicolson, S., and Kumar, S. (2012) Cell death by autophagy: facts and apparent artefacts. *Cell Death Differ. 19*, 87−95.
(180) Raucci, A., Palumbo, R., and Bianchi, M. E. (2007) HMGB1: a signal of necrosis. *Autoimmunity 40*, 285−289.
(181) Zitvogel, L., Kepp, O., and Kroemer, G. (2010) Decoding cell death signals in inflammation and immunity. *Cell 140*, 798−804.
(182) Wang, H., Ward, M. F., and Sama, A. E. (2009) Novel HMGB1-inhibiting therapeutic agents for experimental sepsis. *Stroke 32*, 348−357.
(183) Zhang, J., Takahashi, H. K., Liu, K., Wake, H., Liu, R., Maruo, T., Date, I., Yoshino, T., Ohtsuka, A., Mori, S., and Nishibori, M. (2011) Anti-high mobility group box-1 monoclonal antibody protects the blood-brain barrier from ischemia-induced disruption in rats. *Stroke 42*, 1420−1428.
(184) Gold, L. I., Eggleton, P., Sweetwyne, M. T., Van Duyn, L. B., Greives, M. R., Naylor, S. M., Michalak, M., and Murphy-Ullrich, J. E. (2010) Calreticulin: non-endoplasmic reticulum functions in physiology and disease. *FASEB J. 24*, 665−683.
(185) Obeid, M., Tesenier, A., Ghiringhelli, F., Fimia, G. M., Apetoh, L., Perfettini, J. L., Castedo, M., Mignot, G., Panaretakis, T., Casares, N., Métivier, D., Larochette, N., van Endert, P., Ciccosanti, F., Piacentini, M., Zitvogel, L., and Kromer, G. (2007) Calreticulin exposure dictates the immunogenicity of cancer cell death. *Nat. Med. 13*, 54−61.
(186) Gardai, S. J., McPhillips, K. A., Frasch, S. C., Janssen, W. J., Starefeldt., A., Murphy-Ullrich, J. E., Bratton, D. L., Oldenborg, P. A., Michalak, M., and Henson, P. M. (2005) Cell-surface calreticulin initiates clearance of viable or apoptotic cells through trans-activation of LRP on the phagocyte. *Cell 123*, 321−334.
(187) Zitvogel, L., Kepp, O., Senovilla, L., Menger, L., Chaput, N., and Kroemer, G. (2010) Immunogenic tumor cell death for optimal anticancer therapy: the calreticulin exposure pathway. *Clin. Cancer Res. 16*, 3100−3104.
(188) Jung, K. H., Palik, J. Y., Park, J., Quach, C., Lee, E. J., Choe, Y. S., and Lee, K.-H. (2011) Targeting of calreticulin exposure for optical imaging of etoposide-induced immunogenic tumor cell death. *Mol. Cancer Ther. 10* (Supp.1), B111.
(189) Garg, A. D., Nowis, D., Golab, J., Vandenabeele, P., Krysko, D. V., and Agostinis, P. (2010) Immunogenic cell death, DAMPS and anticancer therapeutics: an emerging amalgamation. *Biochim. Biophys. Acta 1805*, 53−71.
(190) Shay, J. W., and Roninson, I. B. (2004) Hallmarks of senescence in carcinogenesis and cancer therapy. *Oncogene 23*, 2919−2933.
(191) Kuilman, T., Michaloglou, C., Mooi, W. J., and Peeper, D. S. (2010) The essence of senescence. *Genes Dev. 24*, 2463−2479.
(192) Collado, M., and Serrano, M. (2010) Senescence in tumours: evidence from mice and humans. *Nat. Rev. Cancer 10*, 51−57.
(193) Debacq-Chainiaux, F., Erusalimsky, J. D., Campisi, J., and Toussaint, O. (2009) Protocols to detect senescence-associated β-galactosidase (SA-βgal) activity, a biomarker of senescent cells in culture and in vivo. *Nat. Prot. 4*, 1798−1806.
(194) Xue, W., Zender, L., Miething, C., Dickins, R. A., Hernando, E., Krizhanovsky, V., Cordon-Cardo, C., and Lowe, S. W. (2007) Senescence and tumour clearance is triggered by p53 restoration in murine liver carcinomas. *Nature 445*, 656−660.
(195) Tung, C. H., Zeng, Q., Shah, K., Kim, D. E., Schellingerhout, D., and Weissleder, R. (2004) In vivo imaging of β-galactosidase activity using far red fluorescent switch. *Cancer Res. 64*, 1579−1583.
(196) Liu, L., and Mason, R. P. (2010) Imaging β-galactosidase activity in human tumor xenografts and transgenic mice using a chemiluminescent substrate. *PLoS One 5*, e12024.
(197) Van Dort, M. E., Lee, K. C., Hamilton, C. A., Rehemtulla, A., and Ross, B. D. (2008) Radiosynthesis and evaluation of 5-[^{125}I]Iodoindol-3-yl-β-D-galactopyranoside ([^{125}I]IBDG) as a β-galactosidase imaging radioligand. *Mol. Imaging 7*, 187−197.
(198) Louie, A. Y., Hüber, M. M., Ahrens, E. T., Rothbächer, U., Moats, R., Jacobs, R. E., Fraser, S. E., and Meade, T. J. (2000) In vivo visualization of gene expression using magnetic resonance imaging. *Nat. Biotechnol. 18*, 321−325.
(199) Koslowsky, I., Shahhosseini, S., Mirzayans, R., Murray, D., and Mercer, J. (2011) Evaluation of an ^{18}F-labeled oligonucleotide probe targeting p21^{WAF1} transcriptional changes in human tumor cells. *Oncol. Rep. 19*, 265−274.
(200) Ravichandran, K. S. (2011) Beginnings of a good apoptotic meal: the find-me and eat-me signaling pathways. *Immunity 35*, 445−455.
(201) Munoz, L. E., Franz, S., Pausch, F., Fürnrohr, B., Sheriff, A., Vogt, B., Kern, P. M., Baum, W., Stach, C., von Laer, D., Brachvogel, B., Poschl, E., Herrmann, M., and Gaipl, U. S. (2007) The influence on the immunomodulatory effects of dying and dead cells of annexin V. *J. Leukoc. Biol. 81*, 6−14.
(202) Frey, B., Schildkopf, P., Rödel, F., Weiss, E. M., Munoz, L. E., Herrmann, M., Fietkau, R., and Gaipl, U. S. (2009) Annexin A5 renders dead tumor cells immunogenic − implications for multimodal cancer therapies. *J. Immunotoxicol. 6*, 209−216.
(203) Huang, X., Bennett, M., and Thorpe, P. E. (2005) A monoclonal antibody that binds anionic phospholipids on tumor blood vessels enhances the antitumor effect of docetaxel on human breast tumors in mice. *Cancer Res. 65*, 4408−4416.
(204) Beck, A. W., Luster, T. A., Miller, A. F., Holloway, S. E., Conner, C. R., Barnett, C. C., Thorpe, P. E., Fleming, J. B., and Brekken, R. A. (2006) Combination of a monoclonal anti-phosphatidylserine antibody with gemcitabine strongly inhibits the growth and metastasis of orthotopic pancreatic tumors in mice. *Int. J. Cancer 118*, 2639−2643.
(205) He, J., Yin, Y., Luster, T. A., Watkins, L., and Thorpe, P. E. (2009) Antiphosphatidylserine antibody combined with irradiation damages tumor blood vessels and induces tumor immunity in a rat model of gliobastoma. *Clin. Cancer Res. 15*, 6871−6880.
(206) Jinushi, M., Nakazaki, Y., Dougan, M., Carrasco, D. R., Mihm, M., and Dranoff, G. (2007) MFG-E8-mediated uptake of apoptotic cells by APCs links the pro- and antiinflammatory activities of GM-CSF. *J. Clin. Invest. 117*, 1902−1913.
(207) Wang, K., Na, M. H., Hoffman, A. S., Shim, G., Han, S. E., Oh, Y. K., Kwon, I. C., Kim, I. S., and Lee, B. H. (2011) In situ dose amplification by apoptosis-targeted drug delivery. *J. Controlled Release 154*, 214−217.
(208) He, X., Bonaparte, N., Kim, S., Kim, J. H., Aeharya, B., Lee, J. Y., Chi, L., Lee, H. J., Paik, Y. K., Moon, P. G., Baek, M. C., Lee, E. K., Kim, I. S., and Lee, B. H. (2012) Enhanced delivery of t cells to tumor after chemotherapy using membrane-anchored, apoptosis-targeted peptide. *J. Controlled Release*, DOI: 10.1016/j.jconrel.2012.07.023.
(209) Nardella, C., Clohessy, J. G., Alimonti, A., and Pandolfi, P. P. (2011) Pro-senescence therapy for cancer treatment. *Nat. Rev. Cancer 11*, 503−511.
(210) Ewald, J. A., Desotelle, J. A., Wilding, G. W., and Jarrard, D. F. (2010) Therapy-induced senescence in cancer. *J. Natl. Cancer Inst. 102*, 1536−1546.
(211) Castro, R. E., Santos, M. M., Glória, P. M., Ribeiro, C. J., Ferreira, D. M., Xavier, J. M., Moreira, R., and Rodrigues, C. M. (2010) Cell death targets and potential modulators in alzheimer's disease. *Curr. Pharm. Des. 16*, 2851−2864.

(212) Ola, M. S., Nawaz, M., and Ahsan, H. (2011) Role of Bcl-2 family proteins and caspases in the regulation of apoptosis. *Mol. Cell. Biochem. 351*, 41−58.
(213) Fischer, U., and Schulze-Osthoff, K. (2005) Apoptosis-based therapies and drug targets. *Cell Death Differ. 12*, 942−961.
(214) Huang, Q., Li, F., Liu, X., Li, W., Shi, W., Liu, F. F., O'Sullivan, B., He, Z., Peng, Y., Tan, A. C., Zhou, L., Shen, J., Han, G., Wang, X. J., Thorburn, J., Thorburn, A., Jimeno, A., Raben, D., Bedford, J. S., and Li, C. Y. (2011) Caspase 3-mediated stimulation of tumor cell repopulation during cancer radiotherapy. *Nat. Med. 17*, 860−866.
(215) Becattini, B., Sareth, S., Zhai, D., Crowell, K. J., Leone, M., Reed, J. C., and Pellecchia, M. (2004) Targeting apoptosis via chemical design: inhibition of bid-induced cell death by small organic molecules. *Chem. Biol. 11*, 1107−1117.
(216) Hotchkiss, R. S., McConnell, K. W., Bullok, K., Davis, C. G., Chang, K. C., Schwulst, S. J., Dunne, J. C., Dietz, G. P. H., Bähr, M., McDunn, J. E., Karl, I. E., Wagner, T. H., Cobb, J. P., Coopersmith, C. M., and Piwnica-Worms, D. (2006) TAT-BH4 and TAT-Bcl-xL peptides protect against sepsis-induced lymphocyte apoptosis in vivo. *J. Immunol. 176*, 5471−5477.
(217) Kilic, E., Dietz, G. P. H., Hermann, D. M., and Bähr, M. (2002) Intravenous TAT-Bcl-xL is protective after middle cerebral artery occlusion in mice. *Ann. Neurol. 52*, 617−622.
(218) McDunn, J. E., Muenzer, J. T., Dunne, B., Zhou, A., Yuan, K., Hoekzema, A., Hilliard, C., Chang, K. C., Davis, C. G., McDonough, J., Hunt, C., Grigsby, P., Piwnica-Worms, D., and Hotchkiss, R. S. (2009) An anti-apoptotic peptide improves survival in lethal total body irradiation. *Biochem. Biophys. Res. Commun. 355*, 501−507.
(219) You, Z., Savitz, S. I., Yang, J., Degterev, A., Yuan, J., Cuny, G. D., Moskowitz, and Whalen, M. J. (2008) Necrostatin-1 reduced histopathology and improves functional outcome after controlled cortical impact in mice. *J. Cereb. Blood Flow Metab. 28*, 1564−1573.
(220) Northington, F. J., Cavez-Valdez, R., Graham, E. M., Razdan, S., Gauda, E. B., and Martin, L. J. (2011) Necrostatin decreases oxidative damage, inflammation, and injury after neonatal HI. *J. Cereb. Blood Flow Metab. 31*, 178−189.
(221) Zhu, S., Zhang, Y., Bai, G., and Li, H. (2011) Necrostatin-1 ameliorates symptoms in R6/2 transgenic mouse model of Huntington's disease. *Cell Death Dis. 2*, e115.
(222) Weber, W. A. (2009) Assessing tumor response to therapy. *J. Nucl. Med. 50*, 1S−10S.
(223) Wahl, R. L., Jacene, H., Kasamon, Y., and Lodge, M. A. (2009) From RECIST to PERCIST: evolving considerations for PET response criteria in solid tumors. *J. Nucl. Med. 50*, 122S−150S.
(224) Blankenberg, F. G. (2009) Apoptosis imaging: anti-cancer agents in medicinal chemistry. *Anti-Cancer Agent. Med. Chem. 9*, 944−951.